Volume 4, Issue 6 – January – June -2018

ECORFAN

Journal-Democratic Republic of Congo

ISSN-On line: 2414-4924

ECORFAN®

ECORFAN Journal - Democratic Republic of Congo, Volume 4, Issue 6, January-June 2018, is a journal edited semestral by ECORFAN. 6593 Kinshasa 31Rép. DémocratiqueduCongo. WEB: www.ecorfan.org/DemocraticRepublicofCongo/,journal@ecorfan.org. Editor in Chief: RAMOS-ESCAMILLA, María. Co-Editor: ILUNGA-MBUYAMBA, Elisée. MsC. ISSN On line: 2414-4924. Responsible for the latest update of this number ECORFAN Computer Unit. ESCAMILLA-BOUCHÁN, Imelda, LUNA-SOTO, Vladimir, 6593 Kinshasa 31Rép. Démocratique du Congo, last updated June 30, 2018.

ECORFAN-Democratic Republic of Congo

Definition of Journal

Scientific Objectives

Support the international scientific community in its written production Science, Technology and Innovation in the Field of Physical Sciences Mathematics and Earth sciences, in Subdisciplines Image and Signal Processing, Control-Digital System-Artificial, Intelligence-Fuzzy, Logic-Mathematical, Modeling-Computational, Mathematics-Computer, Science.

ECORFAN-Mexico SC is a Scientific and Technological Company in contribution to the Human Resource training focused on the continuity in the critical analysis of International Research and is attached to CONACYT-RENIECYT number 1702902, its commitment is to disseminate research and contributions of the International Scientific Community, academic institutions, agencies and entities of the public and private sectors and contribute to the linking of researchers who carry out scientific activities, technological developments and training of specialized human resources with governments, companies and social organizations.

Encourage the interlocution of the International Scientific Community with other Study Centers in Mexico and abroad and promote a wide incorporation of academics, specialists and researchers to the publication in Science Structures of Autonomous Universities - State Public Universities - Federal IES - Polytechnic Universities - Technological Universities - Federal Technological Institutes - Normal Schools - Decentralized Technological Institutes - Intercultural Universities - S & T Councils - CONACYT Research Centers.

Scope, Coverage and Audience

ECORFAN-Democratic Republic of Congo is a Journal edited by ECORFAN-Mexico S.C in its Holding with repository in Democratic Republic of Congo, is a scientific publication arbitrated and indexed with semester periods. It supports a wide range of contents that are evaluated by academic peers by the Double-Blind method, around subjects related to the theory and practice of Image and Signal Processing, Control-Digital System-Artificial, Intelligence-Fuzzy, Logic-Mathematical, Modeling-Computational, Mathematics-Computer, Science with diverse approaches and perspectives , That contribute to the diffusion of the development of Science Technology and Innovation that allow the arguments related to the decision making and influence in the formulation of international policies in the Field of Physical Sciences Mathematics and Earth sciences. The editorial horizon of ECORFAN-Mexico® extends beyond the academy and integrates other segments of research and analysis outside the scope, as long as they meet the requirements of rigorous argumentative and scientific, as well as addressing issues of general and current interest of the International Scientific Society.

Editorial Board

Arbitration Committee

ZACARIAS - FLORES, José Dionicio. PhD
Centro de Investigación y Estudios Avanzados

JIMENEZ - CONTRERAS, Edith Adriana. PhD
Instituto Politécnico Nacional

VILLASEÑOR - MORA, Carlos. PhD
Universidad Michoacana de San Nicolás de Hidalgo

REYES - RODRÍGUEZ, Aarón Víctor. PhD
Centro de Investigación y Estudios Avanzados

ANZUETO - SÁNCHEZ, Gilberto. PhD
Centro de Investigaciones en Óptica

GUZMÁN - CHÁVEZ, Ana Dinora. PhD
Universidad de Guanajuato

LÓPEZ - MOJICA, José Marcos. PhD
Centro de Investigación y Estudios Avanzados

IBARRA-MANZANO, Oscar Gerardo. PhD
Instituto Nacional de Astrofísica, Óptica y Electrónica

VAZQUEZ - PADILLA, Rita Xóchitl. PhD
Instituto Politécnico Nacional

CONDE - SOLANO, Luis Alexander. PhD
Centro de Investigación y Estudios Avanzados

VÁZQUEZ - LÓPEZ, José Antonio. PhD
Instituto Tecnológico de Celaya

KU - EUAN, Darly Alina. PhD
Centro de Investigación y Estudios Avanzados

JIMÉNEZ - GARCÍA, José Alfredo. PhD
Centro de Innovación Aplicada en Tecnologías Competitivas

CANO - LARA, Miroslava. PhD
Universidad de Guanajuato

CARBALLO - SÁNCHEZ, Álvaro Francisco. PhD
Universidad Autónoma de Puebla

PÉREZ - TORRES, Roxana. PhD
Universidad Tecnológica del Valle de Toluca

SANABRIA - MONTAÑA, Christian Humberto. PhD
Instituto Politécnico Nacional

OROZCO - GUILLÉN, Eber Enrique. PhD
Instituto Nacional de Astrofísica Óptica y Electrónica

TREJO - TREJO, Elia. PhD
Instituto Politécnico Nacional

MARTÍNEZ - BRAVO, Oscar Mario. PhD
Instituto Nacional de Astrofísica, Óptica y Electrónica

ZALDÍVAR - ROJAS, José David. PhD
Centro de Investigación y Estudios Avanzados

GARCÍA - RODRÍGUEZ, Martha Leticia. PhD
Centro de Investigaciones y de Estudios Avanzados

ARCINIEGA - NEVÁREZ, José Antonio. PhD
Universidad Nacional Autónoma de México

BARRAZA - BARRAZA, Diana. PhD
Instituto Tecnológico y de Estudios Superiores de Monterrey

BRICEÑO - SOLIS, Eduardo Carlos. PhD
Centro de Investigación y Estudios Avanzados

PANTOJA - RANGEL, Rafael. PhD
Universidad de Guadalajara

PARADA - RICO, Sandra Evely. PhD
Centro de Investigación y Estudios Avanzados

GARCÍA - GUERRERO, Enrique Efrén. PhD
Centro de Investigación Científica y de Educación Superior de Ensenada

Assignment of Rights

The sending of an Article to ECORFAN-Democratic Republic of Congo emanates the commitment of the author not to submit it simultaneously to the consideration of other series publications for it must complement the Originality Format for its Article.

The authors sign the Authorization Format for their Article to be disseminated by means that ECORFAN-Mexico, S.C. In its Holding Democratic Republic of Congo considers pertinent for disclosure and diffusion of its Article its Rights of Work.

Declaration of Authorship

Indicate the Name of Author and Coauthors at most in the participation of the Article and indicate in extensive the Institutional Affiliation indicating the Department.

Identify the Name of Author and Coauthors at most with the CVU Scholarship Number-PNPC or SNI-CONACYT- Indicating the Researcher Level and their Google Scholar Profile to verify their Citation Level and H index.

Identify the Name of Author and Coauthors at most in the Science and Technology Profiles widely accepted by the International Scientific Community ORC ID - Researcher ID Thomson - arXiv Author ID - PubMed Author ID - Open ID respectively.

Indicate the contact for correspondence to the Author (Mail and Telephone) and indicate the Researcher who contributes as the first Author of the Article.

Plagiarism Detection

All Articles will be tested by plagiarism software PLAGSCAN if a plagiarism level is detected Positive will not be sent to arbitration and will be rescinded of the reception of the Article notifying the Authors responsible, claiming that academic plagiarism is criminalized in the Penal Code.

Arbitration Process

All Articles will be evaluated by academic peers by the Double Blind method, the Arbitration Approval is a requirement for the Editorial Board to make a final decision that will be final in all cases. MARVID® is a derivative brand of ECORFAN® specialized in providing the expert evaluators all of them with Doctorate degree and distinction of International Researchers in the respective Councils of Science and Technology the counterpart of CONACYT for the chapters of America-Europe-Asia-Africa and Oceania. The identification of the authorship should only appear on a first removable page, in order to ensure that the Arbitration process is anonymous and covers the following stages: Identification of the Journal with its author occupation rate - Identification of Authors and Coauthors - Detection of plagiarism PLAGSCAN - Review of Formats of Authorization and Originality-Allocation to the Editorial Board- Allocation of the pair of Expert Arbitrators-Notification of Arbitration - Declaration of observations to the Author-Verification of Article Modified for Editing-Publication.

Instructions for Scientific, Technological and Innovation Publication

Knowledge Area

The works must be unpublished and refer to topics of Image and Signal Processing, Control-Digital System-Artificial, Intelligence-Fuzzy, Logic-Mathematical, Modeling-Computational, Mathematics-Computer, Science and other topics related to Physical Sciences Mathematics and Earth sciences.

Presentation of Content

In Volume 4 Issue 6, as a first article we present, *Global variable-structure controller applied to the degree of freedmon manipulators robots with rotational flexible joint*, by CHAVEZ-GUZMAN, Carlos Alberto, PEREZ-GARCIA, Alejandro, ESQUEDA-ELIZONDO, Jose Jaime and MERIDA-RUBIO, Jovan Hosea, with adscription at the Universidad Autónoma de Baja California, as a second article we present, Continuous *Twisting apply to a nonlinear mathematical model of sinchronous generato*r, by RAMIREZ-YOCUPICIO, Susana, RUIZ-IBARRA, Joel, PALACIO- FIVE, Ramón René and RUIZ-IBARRA, Erica, with adscription at the Instituto Tecnológico de Sonora, as the third article we present, *Development of an application for monitoring the level of a fluid, using a cell phone, Bluetooth communication and Arduino platform*, by GUTIERREZ -GRANADOS, Cuitláhuac, ESPINOSA-AHUMADA, Elias and HERNÁNDEZ-TOVAR, Jonathan, with secondment at the Technological University of San Juan del Río, as fourth article we present, *Design and implement a solar tracker control algorithm for a photovoltaic module*, by AVALOS-GALINDO, Carlos David, ONTIVEROS-MIRELES, Joel Josué, GALÁN-HERNÁNDEZ, Néstor Daniel and RUBIO-ASTORGA, Guillermo Javier, with adscription in the Instituto Tecnológico de Culiacán.

Content

Article **ECORFAN Journal Democratic Republic of Congo**
June 2018 Vol.4 No.6 1-10

Global variable-structure controller applied to *l* degree of freedmon manipulators robots with rotational flexible joint

Controlador global de estructura variable para un robot manipulador de *l* grados de libertad con articulaciones rotacionales y flexible

CHAVEZ-GUZMAN, Carlos Alberto†*, PEREZ-GARCIA, Alejandro, ESQUEDA-ELIZONDO, Jose Jaime and MERIDA-RUBIO, Jovan Oseas

Universidad Autónoma de Baja California, Facultad de Ingeniería y Negocios

ID 1st Author: *Carlos Alberto, Chavez-Guzman* / **ORC ID**: 0000-0002-2850-3676, **CVU CONACYT ID**: 94692

ID 1st Coauthor: *Alejandro, Perez-Garcia* / **ORC ID**: 0000-0001-9556-9125

ID 2nd Coauthor: *Jose Jaime, Esqueda-Elizondo* / **ORC ID**: 0000-0001-8710-8978, **Researcher ID Thomson**: I-2941-2017, **CVU CONACYT ID**: 90966

ID 3rd Coauthor: *Jovan Oseas, Merida-Rubio* / **ORC ID**: 0000-0002-9355-4787, **CVU CONACYT ID**: 234759

Received January 18, 2018; Accepted June 20, 2018

Abstract

In this work is proposed a methodology for a global variable-structure controller (GVSC) applied to nonlinear, time-varying and underactuated systems affected by both matched and unmatched perturbations, the main idea is designed a GVSC with an integral sliding mode control coupled together with a nonlinear $\mathcal{H}_\infty$ control. It is theoretically proven that, using the proposed controller, the trajectories of the states in the feedback loop systems are forced to stay into the sliding mode and reject the coupled perturbations by the integral sliding mode control, and the stability of feedback loop system into the switching mode and the attenuated uncoupled perturbations are done by nonlinear $\mathcal{H}_\infty$ control. This structure is used to solve the trajectory tracking problem in the *l* degrees of freedom (DOF) manipulators robots with flexible and rotational joints. The performance issues of the GVSC are illustrated in simulation studies made for a three-DOF robot manipulator.

Robust control, Nonlinear systems, Manipulator robots

Resumen

Se propone la metodología del diseño de un controlador global de estructura variable (CGEV) compuesto de un control por modo deslizante integral en combinación de un control $\mathcal{H}_\infty$ no lineal para sistemas no lineales, subactuados y variantes en el tiempo afectado por perturbaciones acopladas y no acopladas. La finalidad de la estructura propuesta es que el control por modo deslizante integral mantenga las trayectorias de los estados del sistema en lazo cerrado dentro del modo deslizante y rechace las perturbaciones acopladas y el control $\mathcal{H}_\infty$ no lineal garantice la estabilidad del sistema en lazo cerrado dentro del modo deslizante y atenué las perturbaciones no acopladas. La validación de la estructura de control propuesta se realiza a través de la simulación de un ejemplo numérico que resuelve el problema de regulación de movimiento en un robot manipulador de *l* grados de libertad (GDL), con articulaciones rotacionales que presenta el efecto de elasticidad.

Control robusto, Sistemas no lineales, Robots manipuladores

Citation: CHAVEZ-GUZMAN, Carlos Alberto, PEREZ-GARCIA, Alejandro, ESQUEDA-ELIZONDO, Jose Jaime and MERIDA-RUBIO, Jovan Oseas. Global variable-structure controller applied to l degree of freedmon manipulators robots with rotational flexible joint**.** ECORFAN Journal-Democratic Republic of Congo 2018, 4-6: 1-10.

* Correspondence to Author (email: cchavez@uabc.edu.mx)
† Researcher contributing first author.

Introduction

This paper deals with the analysis and design of a global control of variable structure (CGEV) based on the control by integral sliding mode in combination with the control H_∞ for nonlinear systems varying in time affected by both coupled and uncoupled perturbations . As a case study will solve the problem of regulation of movement in a robot manipulator of degrees of freedom with rotational joints that have the undesired effect of elasticity in each of them, as well as the effect of the mentioned disturbances.

Regarding this line is the work of Utkin, (1992) with the control by sliding mode that has been used successfully when there is uncertainty in the parameters and to reject coupled external disturbances, besides concluding stability in finite time, the stability of the system In closed loop it is only guaranteed when its dynamic enters the sliding mode, however, the drawback of this controller is the effect of chattering in the control signal.

The control by integral sliding mode appears in the decade of the 90's (Utkin, Guldner and Shi, 2009) present the advantages of the control by sliding mode, and solve the problem of the reach to the surface with a function that guarantees that the dynamics of the system in closed loop initiate and stay in it, in addition to reducing the effect of chattering on the control signal due to the integrator.

In Wen and Jian, (2001) an integral sliding mode control is proposed in combination with an optimal quadratic linear regulator for nonlinear systems that vary in time in the presence of uncoupled perturbations and its main contribution was to propose the variant sliding function in the time and show that the uncoupled disturbances remain in the sliding mode for all time.

In Castaños and Fridman, (2009) continue with the previous work, providing new elements such as separating the disturbances into coupled and uncoupled and propose a controller H_∞ locally for the nominal control in order to attenuate the uncoupled disturbances.

In Rubagotti, Castaño, Ferrara and Fridman, (2011) and Fridman, Barbo, Plestan, (2016) and Galvan and Fridman (2015) extend the last two works by proposing a sliding function where the projection matrix varies according to the states of the system and recently is the work of Miranda, Chavez and Aguilar, (2017) in it proposes a variable structure control composed of a sliding mode control and a non-linear H_∞ control for a mechanical system of a rotational articulation with the elasticity effect. Based on the previous work we propose a global variable structure controller that solves the problem of regulation of movement of the manipulator arm of l degrees of freedom and also attenuated the effects of coupled and uncoupled disturbances.

The present article is organized as follows: section II provides the characteristics of the plant and the global control of variable structure analyze, section II presents the design of the CGEV in general form for a non-linear system variant with the time and not autonomous, section III is designed the CGEV for the case of a robot manipulator of degrees of freedom with rotational and flexible articulations that present coupled and uncoupled perturbations and validates the theory with a practical case of a mechanical system of a degree of freedom in MatLab / Simulink, finally the results obtained and the conclusions are presented.

1. Problem Statement

Consider the following nonlinear and variant time system of the form:

$$\dot{x} = f(x,t) + g_2(x,t)(u + w_m) + g_2^{\perp}(x,t)w_u \quad (1)$$

where $t \in \mathbb{R}^+$ represents the time, $x(t) \in \mathbb{R}^n$ is the state vector, $u(t) \in \mathbb{R}^m$ is the control input vector, $w_m(t) \in \mathbb{R}^m$, $w_u(t) \in \mathbb{R}^{nm}$ are coupled and uncoupled perturbations respectively, uncoupled perturbations are assumed to belong to the space $L_2^e(0, T)$ where (Khalil, 2015)

$$\mathcal{L}_2^e(0,T) = \int_0^T \|w_u(t)\|^2 dt < \infty$$

and considering that both disturbances are bounded by:

$$\|w_m(t)\|_\infty \leq W_m^+, \ \|w_u(t)\|_\infty \leq W_u^+ \quad (2)$$

ISSN: 2414- 4924

W_m^+ and W_u^+ they are constants that are known a priori. The functions $f\ (x,\ t)$ and $g_2\ (x,\ t)$ are assumed to be continuous to sections in t for all x and continuously differentiable in x for all t. Sea la función matricial $g_2^{\perp}(x,t) \in \mathbb{R}^{n\times(n-m)}$ of full column range that is the orthogonal complement of g_2 (x, t) such that $g_2^T(x,t)g_2^{\perp}(x,t) = 0$ for all x and all t (Fridman, 2014). The system (1) satisfies the following assumption.

Assumption 1. Be the rank$(g_2(x,t)) = m$ for all $(x,t) \in \mathbb{R}^n \times \mathbb{R}^+$.

If the above assumption is fulfilled then the law of global control of variable structure for the system (1) of the form is proposed:

$$u(t) = u_s(t) + u_1(t) \tag{3}$$

where u_s (t) is the control in the sliding mode responsible for the trajectories converging to the origin while the uncoupled perturbations w_u (t) are attenuated and u_1 (t) is the control by integral sliding mode which incorporates an integrator in the control discontinuous and its function is to reject the coupled perturbations w_m (t) and to prevent the system trajectories from leaving the sliding mode.

2. Design of the CGEV

The design of the CGEV is developed in two stages, the first consists of the design of the control by integral sliding mode and the second of the controller H_∞ non-linear.

2.1. Control design by integral sliding mode

Consider the following sliding surface for the disturbed system (1) of the form

$$s(x,t) = D\left((x(t) - x(t_0) - \int_{t_0}^{t}(f(x_s,t) + g_2(x_s,t)u_s)dt\right) \tag{4}$$

where $D \in \mathbb{R}^{m\times n}$ it is a constant matrix and $x_s(t) \in \mathbb{R}^n$ it is the vector of states in the sliding mode. The sliding function s (x, t) represents the difference between the trajectories of the disturbed system (1) and of the plant in the sliding mode weighted by the matrix D. It is notable to note that the sliding mode starts with the initial condition, that is, $t = t_0, s(x,t) = 0$. It is assumed that the system (1) satisfies the following assumption.

Assumption 2. Let Dg_2 (x, t) be uniformly invertible for all $(x,t) \in \mathbb{R}^n \times \mathbb{R}^+$.

If assumption 2 is satisfied, then the control by integral sliding mode is of the form

$$u_1(t) = -\Gamma\, Sign(s(x,t)) \tag{5}$$

where $Sign(s(x,t)) = [sign(s_1), sign(s_2), \cdots, sign(s_m)]^T$, and the sign function is defined in the way:

$$sign(s) = \begin{cases} 1 & yes \quad s > 0 \\ 0 & yes \quad s = 0 \\ -1 & yes \quad s < 0 \end{cases}$$

Regarding the control gain by integral sliding mode, it is subject to:

$$\Gamma > W_m^+ + \frac{\|g_2^{\perp}(x,t)\|}{\|g_2(x,t)\|}W_u^+ \tag{6}$$

where $\|\cdot\|$ refers to the Euclidean norm. The gain (6) is to force the trajectories of the system (1) not to leave the sliding surface $s(x,t) = 0$.

2.1.1. Equivalent control

The analysis of the equivalent control u_{1eq} (Utkin, 1992) is obtained by making $s(x,t) = \dot{s}(x,t) = 0$, that is

$$\dot{s} = Dg_2(x,t)(u_1 + w_m) + Dg_2^{\perp}(x,t)w_u = 0$$

Clear $u_1(t)$ and make $u_1 \to u_{1eq}$ in the previous equation you have to

$$u_{1eq} = -w_m - \left(Dg_2(x,t)\right)^{-1}Dg_2^{\perp}(x,t)w_u.$$

Substituting the equation (7) in (1) the following system is obtained in the sliding mode:

$$\dot{x}_s = f(x_s,t) + g_2(x_s,t)u_s + \Big(I - g_2(x_s,t)\left(Dg_2(x_s,t)\right)^{-1}D\Big)g_2^{\perp}(x_s,t)w_u, \tag{8}$$

where $\dot{x}_s \in \mathcal{S} = \{x \in \mathbb{R}^n : s(x,t) = 0\}$. Note that the uncoupled disturbances remain in the plant in the sliding mode which motivates the use of the non-linear H_∞ control to attenuate its effects.

ISSN: 2414- 4924

2.2. Control design H_∞ non-linear

Once the trajectories are in the domain of $\mathcal{S}$, then the system (8) takes the form

$$\dot{x}_s = f(x_s,t) + g_2(x_s,t)u_s + \underbrace{\left(I - g_2(x_s,t)\left(Dg_2(x_s,t)\right)^{-1}D\right)g_2^{\perp}(x_s,t)}_{g_3(x_s,t)} w_u(t) \quad (9)$$

$$z = h_1(x_s,t) + k_{12}(x_s,t)u_s$$

$$y = h_2(x_s,t)$$

where $z(t) \in \mathbb{R}^s$ is the vector of the unknown output to be controlled, $y(t) \in \mathbb{R}^n$ it is the output vector available for system measurement. It is assumed that the system (9) satisfies the following assumptions:

Assumption 3. Functions f, g_2, g_3, h_1, h_2 and k_{12} are assumed to be continuous at t, continuously differential at x_s and of appropriate dimensions.

Assumption 4. Let $f(0,t) = 0, h_1(0,t) = 0$, y $h_2(0,t) = 0$ for all ≥ 0 .

Assumption 5. Let $h_1^T k_{12} = 0$, $k_{12}^T k_{12} = I$ se must satisfy for all $(x_s,t) \in \mathbb{R}^n \times \mathbb{R}^+$.

Assumption 3 ensures that the dynamics of the system are well positioned, while the system is excited with external inputs. Assumption 4 ensures that the origin is the only equilibrium point in the absence of inputs u_s (t) = 0 and disturbances w_u (t) = 0 for the dynamic system (9). Assumption 5 is related to numerical advantages considered in the H_∞ standard control problem (Orlov, 2014).

The law of control

$$u_s(t) = K(x_s,t) \quad (10)$$

It is a globally admissible driver by feedback of states if the closed loop system (9) and (10) is asymptotically stable globally as long as $w_u = 0$. The gain $\mathcal{L}_2$ of the system (9) is less than γ if the response of z (t), result of w_u (t) for a vector of initial states x_s (0) = 0 satisfies the following inequality

$$\int_{t_0}^{t_1} \|z(t)\|^2 dt < \gamma^2 \int_{t_0}^{t_1} \|w_u(t)\|^2 dt \quad (11)$$

For all $t_1 > t_0$ and every function continues in sections $w_u(t)$. A permissible local controller (10) constitutes a local solution to the control problem H_∞ if there is a region U around the equilibrium point such that the inequality (11) is satisfied for all $t_1 > t_0$ and a continuous function with stretches w_u (t) for which the trajectories of the states of the closed loop system start at the point given by the vector x_s (0) = 0 and remain in U for all $t \in [t_0, t_1]$ (Isidori y Astol, 1992).

Next, the hypothesis under which the solution to the problem of control is given is presented $\mathcal{H}_\infty$.

Hypothesis 1 (Orlov, 2014). There is a positive definite function F (x_s, t) and a soft definite positive function V (x_s, t) such that the inequality of Hamilton-Jacobi-Isaacs

$$\frac{\partial V}{\partial t} + \frac{\partial V}{\partial x_s} f + \gamma^2 \alpha_1^T \alpha_1 - \alpha_2^T \alpha_2 + h_1^T h_1 + F \leq 0 \quad (12)$$

it is fulfilled with

$$\alpha_1(x_s,t) = \frac{1}{2\gamma^2} g_3^T(x_s,t)\left(\frac{\partial V(x_s,t)}{\partial x_s}\right)^T$$

$$\alpha_2(x_s,t) = -\frac{1}{2} g_2^T(x_s,t)\left(\frac{\partial V(x_s,t)}{\partial x_s}\right)^T.$$

Given hypothesis 1 the following theorem is postulated:

Theorem 1 (Orlov, 2014). Assume that hypothesis 1 is valid. Then a solution to the control problem H_∞ is given for the closed loop system (9) through the law of control by feedback of states

$$u_s(t) = \alpha_2(x_s,t) \quad (13)$$

which stabilizes asymptotically the system free of disturbances (9) and makes the gain L_2 of the system in the sliding mode (9) is smaller than γ.

Figure 1 shows the block diagram of a feedback system based on the CGEV composed of the integral sliding mode control and the non-linear H_∞ control applied to a non-linear and non-autonomous plant with coupled and uncoupled perturbations, where $x_d(t) \in \mathbb{R}^n$ is the vector of desired states.

ISSN: 2414- 4924

2.2.1. System stability analysis

The stability of the system in closed loop (1), (3) is demonstrated in the theorem of Miranda, Chavez and Aguilar, (2017), which raises the following: be the assumptions 3-5 and hypothesis 1 satisfied and be the system non-linear (1) with the control (5) that satisfies (9) next to the control H_∞ (13). Then the equilibrium point of the closed loop system (1), (5) and (13) is asymptotically stable and the gain L_2 of the system in the sliding mode is less than γ in the presence of disturbances that satisfy (2).

I. Case study: Track tracking problem for a robot with flexible joints

The elasticity effect is very common in manipulator robots, this phenomenon occurs when the movement of the actuator is transmitted to the articulation by means of toothed belts, chains, cables, use of gears, cyclo reducers, Harmonic Drive reducers, etc. all these elements introduce a variation in displacement with respect to time, that is why it is necessary, according to (Rivin, 1985), to incorporate the elasticity effect in the dynamic model of the robot, coupled with this phenomenon we have the uncoupled perturbations that are present as external disturbances, which affects the performance of the system in closed loop.

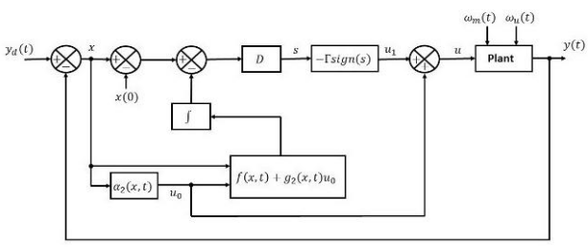

Figure 1 Global control of variable structure
Source: Self Made

The system under study, governed by the following differential equations (Spong and Vidyasagar, 1989):

$$M(q)\ddot{q} + C(q,\dot{q})\dot{q} + g(q) + K(q-\theta) + w_u = 0 \quad (14)$$

$$J\ddot{\theta} - K(q-\theta) = \tau + w_m$$

Where $q(t) \in \mathbb{R}^l$ is the joint position vector, $\dot{q}(t) \in \mathbb{R}^l$ is the joint velocity vector, $\theta(t) \in \mathbb{R}^l$ is the position vector of the actuator, and due to the elasticity effect $q(t) \neq \theta(t)$ while the mechanism is in motion, $M(q) \in \mathbb{R}^{l\times l}$ is a positive definite symmetric matrix that represents the inertial matrix, $C(q,\dot{q}) \in \mathbb{R}^{l\times l}$ is the matrix of centrifugal and Coriolis forces, $g(q) \in \mathbb{R}^l$ is the vector of gravitational torque, $K \in \mathbb{R}^{l\times l}$ is a positive definite symmetric matrix that represents the torsional constants of flexible joints $(K = diag\{k_1, k_2, \cdots, k_l\})$, $J \in \mathbb{R}^{l\times l}$ is a positive definite symmetric matrix that contains in its main diagonal the product of the moments of inertia of the engine (j_i) by the square of the ratio of turns of the transmission (r_i), that is to say $J = diag\{j_1 r_1^2, j_2 r_2^2, \cdots, j_l r_l^2\}$, $\tau(t) \in \mathbb{R}^l$ is the vector of forces and pairs applied to the joints and $w_u(x,t), w_m(t) \in \mathbb{R}^l$ They denote uncoupled and coupled disturbances respectively due to the uncertainty of the model or external disturbances. Equation (14) represents a mechanical system with flexible joints subject to coupled and uncoupled disturbances.

1.1. Control objective

The trajectory tracking problem of the manipulator robot with flexible joints (14) is established in the following way: given a limited set of functions $q_d(t), \dot{q}_d(t), \ddot{q}_d(t) \in \mathbb{R}^l$ referred to as desired joint positions, velocities and accelerations, respectively; The objective of control is to ensure the global asymptotic stability of the equilibrium point of the closed loop system, ie

$$\lim_{t\to\infty} \|q(t) - q_d(t)\| = 0 \quad (15)$$

for any arbitrary initial condition $q(0) \in \mathbb{R}^l$, and for the disturbance-free system (14), finally, the gain L_2 of the disturbed system in the sliding mode is satisfied is less than γ with respect to the output $z(t)$.

1.2. Design of the CGEV for the manipulator robot

The representation in state variables of the system (14) in terms of errors is given by

$$\dot{e}_1 = e_2 \quad (16)$$

ISSN: 2414- 4924

$\dot{e}_2 = M(e_1 + q_d)^{-1}[M(e_1 + q_d)\ddot{q}_d - C(e_1 + q_d, e_2 + \dot{q}_d)(e_2 + \dot{q}_d) - g(e_1 + q_d) - K(e_1 + q_d - \theta) - w_u]$
$\dot{e}_3 = e_4$
$\dot{e}_4 = J^{-1}\left[-J\ddot{\theta}_d + K(e_1 + q_d - \theta) + \tau + w_m\right]$

where $e_1(t) = q(t) - q_d(t)$ is the error vector of joint positions, $e_2(t) = \dot{q}(t) - \dot{q}_d(t)$ is the error vector of joint velocities, $e_3(t) = \theta(t) - \theta_d(t)$ is the vector of errors positions of the actuator and finally $e_4(t) = \dot{\theta}(t) - \dot{\theta}_d(t)$ is the actuator speed error vector.

Decoupling the states of the system (16) facilitates the synthesis of the control H_∞, therefore, a virtual control entry is proposed according to the regular form of Utkin, (1992) within the state $\theta(t) = \eta(t) + \theta_d(t)$, and you get the solution based on the virtual control η de $\dot{e} = 0$, as:

$$\eta(t) = K^{-1}[M(q_d)\ddot{q}_d + C(q_d, \dot{q}_d)\dot{q}_d + g(q_d)] + q_d - \theta_d - K_{p1}e_1 - K_{d1}e_2 \quad (17)$$

The earnings $K_{p1} = K_{p1}^T > 0$ y $K_{d1} = K_{d1}^T > 0$ they assure that the states $(e_1, e_2)^T \to 0$ when $t \to \infty$. Finally, a coordinate change is made with the function $\sigma = e_3 - \eta$ which is derived continuously until the control input τ of the form appears $\ddot{\sigma} = \dot{e}_4 - \ddot{\eta}$ and doing what $\dot{e}_4 - \ddot{\eta} = 0$ is obtained

Proposition 3. Shape stabilizer control:

$$\tau(t) = J\left(\ddot{\eta} + \ddot{\theta}_d\right) - K(x_1 + q_d - \eta - \theta_d) - K_{p2}x_3 - K_{d2}x_4 + u \quad (18)$$

Where the new states are $x_1 = e_1$, $x_2 = e_2$, $x_3 = \sigma$, $x_4 = \dot{\sigma}$ y $\theta_d(t), \dot{\theta}_d(t), \ddot{\theta}_d(t) \in \mathbb{R}^l$ are the desired angle, speed and acceleration of the motor, respectively; $u(t)$ is the global control defined in (3) y $K_{p2} = K_{p2}^T > 0$ y $K_{d2} = K_{d2}^T > 0$.

The representation of the system in closed loop in terms of the new defined states x (t) that are obtained by substituting (17) and (18) in (16), is given by

$$\dot{x}_1 = x_2 \quad (19)$$
$\dot{x}_2 = M(x_1 + q_d)^{-1}\left[-h(x,t) - C(x_1 + q_d, x_2 + \dot{q}_d)x_2 - \left(K\ K_{p1}\right)x_1 - K\ K_{d1}x_2 + w_u\right]$
$\dot{x}_3 = x_4$
$\dot{x}_4 = J^{-1}\left[-K_{p2}x_3 - K_{d2}x_4 + u + w_m\right]$

where $h(x,t) = [M(x_1 + q_d) - M(q_d)]\ddot{q}_d + [C(x_1 + q_d, x_2 + \dot{q}_d) - C(q_d, \dot{q}_d)]\dot{q}_d + g(x_1 + q_d) - g(q_d)$.

The feedback system is decoupled in two sections (one mechanical and one actuator) with a control input τ, and its origin in $x_0 = 0 \in \mathbb{R}^n$ it will be a unique balance point if and only if

$$\lambda_{min}\{K_{p1}\} > \frac{K_g + K_M\|\ddot{q}_d\| + K_{c2}\|\dot{q}_d\|^2 - \lambda_{min}\{K\}}{\lambda_{min}\{K\}} \quad (20)$$

The discontinuous control (5) is designed from (19) where

$$f(x,t) = \begin{bmatrix} x_2 \\ x_\psi \\ x_4 \\ J^{-1}\left[-K_{p2}x_3 - K_{d2}x_4\right] \end{bmatrix} \quad (21)$$

with $x_\psi = M(x_1 + q_d)^{-1}\left[-h(x,t) - C(x_1 + q_d, x_2 + \dot{q}_d)x_2 - \left(K + K_{p1}\right)x_1 - K\ K_{d1}x_2\right]$, and the functions

$$g_2(x,t) = \begin{bmatrix} 0 \\ 0 \\ 0 \\ J^{-1} \end{bmatrix},\ g_2^{\perp}(x,t) = \begin{bmatrix} 0 \\ M(x_1 + q_d)^{-1} \\ 0 \\ 0 \end{bmatrix} \quad (22)$$

Based on the system (8) where the expression is defined

$$\left(I - g_2(x_s,t)\left(Dg_2(x_s,t)\right)^{-1}D\right)g_2^{\perp}(x_s,t)$$

and by substituting D = [0,0,0, J], then the representation on the sliding surface is reduced to the form:

$$\dot{x}_s = f(x_s,t) + g_2(x_s,t)u_s + g_2^{\perp}(x_s,t)w_u \quad (23)$$

where the u_s control is designed through the non-linear H_∞ control technique. The target output for the motion regulation problem is proposed

$$z = \begin{bmatrix} u_s \\ \rho\ tanh(x_{s1}) \\ \rho\ x_{s2} \\ \rho\ tanh(x_{s3}) \\ \rho\ x_{s4} \end{bmatrix} \quad (24)$$

where ρ is a positive constant and $\tanh(x_{si}), i = 1,3$, it is the hyperbolic tangent function. The position and speed of the articulation and the actuator are available for feedback.

ISSN: 2414- 4924

$$y = x_s \quad (25)$$

while equations (21) - (22), (24) - (25) are represented in the generalized form (23) and the remaining functions of the form (9) are:

$$h_1 = \rho \begin{bmatrix} 0 \\ tanh(x_{s1}) \\ x_{s2} \\ anh(x_{s3}) \\ x_{s4} \end{bmatrix}, h_2 = x_s, K_{12} = \begin{bmatrix} I \\ 0 \end{bmatrix} \quad (26)$$

The vector and matrix functions of the system (23) are of appropriate dimension.

Theorem 2. Assumptions 3-5 and hypothesis 1 satisfied under the following functions

$$V(x_s,t) = \frac{1}{2}x_{s1}^T\left(K + K\,K_{p1}\right)x_{s1} + \frac{1}{2}x_{s2}^T M(x_{s1}+q_d)x_2 + \beta tanh(x_{s1})^T M(x_{s1}+q_d)x_{s2} + \frac{1}{2}x_{s3}^T K_{p2}x_{s3} + \frac{1}{2}x_{s4}^T J x_{s4} + \gamma tanh(x_{s3})^T J x_{s4} \quad (27)$$

$$F(x_s) = \epsilon \tanh(x_{s1})^T \tanh(x_{s1}) + \epsilon\, x_{s2}^T x_{s2} + \epsilon \tanh(x_{s3})^T \tanh(x_{s3}) + \epsilon\, x_{s4}^T x_{s4} \quad (28)$$

with $\beta > 0$, $\gamma > 0$ and then $V(x_s,t)$ it will be defined positive for all $x_s \in \mathbb{R}^n$ and radially desacoted if and only if

$$\lambda_{max}\{K_{p2}\} > \gamma^2\lambda_{max}\{J\},$$
$$\lambda_{min}\{K_{p2}\} > \gamma^2\lambda_{min}\{J\}. \quad (29)$$

is fulfilled. In addition, the Hamilton-Jacobi-Isaacs inequality is satisfied if

$$\lambda_{min}\{K_{p1}\} > \frac{(0.5\beta K_{c1}\|\dot{q}_d\| + 0.5K_{h2} + 0.5\beta K_{h1} + 0.5a_1)^2 + K_{h2} + \frac{1}{\beta}(\rho^2+\epsilon)}{a_2 + \beta^2\lambda_{max}\{M(x_1+q_d)\} - \beta^2\sqrt{n}K_{c1} - \beta K_{h1} - \beta(\rho^2+\epsilon)} > \frac{\beta K_{h2} + \rho^2 + \epsilon - \beta\lambda_{min}\{K\}}{\beta\lambda_{min}\{K\}} \quad (30)$$

$$\lambda_{min}\{K_{p1}\} > \frac{\beta\lambda_{max}\{M(x_1+q_d)\} + \beta\sqrt{n}K_{c1} + K_{h1} + \rho^2 + \epsilon}{\lambda_{min}\{K\}} \quad (31)$$

$$\lambda_{min}\{K_{p2}\} > \frac{0.25\gamma\lambda_{max}^2\{K_{d2}\}}{\lambda_{min}\{K_{d2}\} - \gamma\lambda_{max}\{J\} - \rho^2 - \epsilon} + \frac{\rho^2+\epsilon}{\gamma} \quad (32)$$

$$\lambda_{min}\{K_{d2}\} > \gamma\lambda_{max}\{J\} + \rho^2 + \epsilon \quad (33)$$

where $a_1 = \beta\lambda_{max}\{K\}\lambda_{max}\{K_{d1}\}$, $a_2 = \beta\lambda_{min}\{K\}\lambda_{min}\{K_{d1}\}$, $\epsilon > 0$ it is a sufficiently small constant. So based on Theorem 1 the law of control by feedback of states is

$$u_s(t) = \alpha_2(x_s,t) = -\frac{1}{2}[\gamma \tanh(x_{s3}) + x_{s4}] \quad (34)$$

stabilizes the equilibrium point in asymptotic and global form of the disturbance-free system (23) and (34) will ensure that the gain L_2 of the closed-loop system is less than γ.

Proof. It is proposed to separate the inequality of Hamilton-Jacobi-Isaacs (12) into two parts, that is to say

$$H(x_s,t) = H_1(x_s,t) + H_2(x_s,t)$$

Where

$$H_1(x_s,t) = \frac{\partial V}{\partial t} + \frac{\partial V}{\partial x_s}f + h_1^T h_1 + F$$
$$H_2(x_s,t) = \gamma^2\alpha_1^T\alpha_1 - \alpha_2^T\alpha_2$$

$H_1(x_s,t)$, $H_2(x_s,t)$ are developed and we get their maximum levels

$$H_1(x_s,t) \le \beta\lambda_{max}\{M(x_{s1}+q_d)\}\|x_{s2}\|^2 - \lambda_{min}\{K\}\lambda_{min}\{K_{d1}\}\|x_{s2}\|^2 - \beta\lambda_{min}\{K + K\,K_{p1}\}\|\tanh(x_{s1})\|^2 + \gamma\lambda_{max}\{J\}\|x_{s4}\|^2 - \lambda_{min}\{K_{d2}\}\|x_{s4}\|^2 - \gamma\lambda_{min}\{K_{p2}\}\|\tanh(x_{s3})^T\|^2 + \beta K_{c1}\|x_{s2}\|^2 + \beta K_{c1}\|\dot{q}_d\|\|\tanh(x_{s1})\|\|x_{s2}\|^2 + K_{h1}\|x_{s2}\|^2 + K_{h2}\|\tanh(x_{s1})\|\|x_{s2}\| + \beta K_{h1}\|\tanh(x_{s1})\|\|x_{s2}\| + \beta K_{h2}\|\tanh(x_{s1})\|^2 + \beta\lambda_{max}\{K\}\lambda_{max}\{K_{d1}\}\|\tanh(x_{s1})\|\|x_{s2}\| + \gamma\lambda_{max}\{K_{d2}\}\|\tanh(x_{s3})\|\|x_{s4}\| + (\rho^2+\epsilon)\|\tanh(x_{s1})\|^2 + (\rho^2+\epsilon)\|x_{s2})\|^2 + (\rho^2+\epsilon)\|\tanh(x_{s3})\|^2 + (\rho^2+\epsilon)\|x_{s4})\|^2$$

The inequalities of vector functions of secant and hyperbolic tangent and their properties were considered (Kelly, Santibañez and Loria, 2005). The previous inequality can be represented as follows

$$H_1(x_s,t) \le -\begin{bmatrix} \|\tanh(x_{s1})\| \\ \|x_{s2}\| \\ \|\tanh(x_{s3})\| \\ \|x_{s4}\| \end{bmatrix}^T Q_1 \begin{bmatrix} \|\tanh(x_{s1})\| \\ \|x_{s2}\| \\ \|\tanh(x_{s3})\| \\ \|x_{s4}\| \end{bmatrix}$$

ISSN: 2414- 4924

$$Q_1 = \begin{bmatrix} q_{1\_11} & q_{1\_12} & 0 & 0 \\ q_{1\_12} & q_{122} & 0 & 0 \\ 0 & 0 & q_{1\_33} & q_{1\_34} \\ 0 & 0 & q_{1\_34} & q_{1\_44} \end{bmatrix} \quad (35)$$

where:

$q_{1\_11} = \beta\lambda_{min}\{K + K\,K_{p1}\} - \beta K_{h2} - \rho^2 - \epsilon$
$q_{1\_12} = -0.5\beta K_{c1}\|\dot{q}_d\| - 0.5K_{h2} - 0.5\beta K_{h1} - 0.5\beta\lambda_{max}\{K\}\lambda_{max}\{K_{d1}\}$
$q_{1\_22} = \lambda_{min}\{K\}\lambda_{min}\{K_{d1}\} - \beta\lambda_{max}\{M(x_{s1} + q_d)\} - \beta K_{c1}\sqrt{n} - K_{h1} - \rho^2 - \epsilon$
$q_{1\_33} = \gamma\lambda_{min}\{K_{p2}\} - \rho^2 - \epsilon$
$q_{1\_34} = -0.5\gamma\lambda_{max}\{K_{d2}\}$
$q_{1\_44} = \lambda_{min}\{K_{d2}\} - \gamma\lambda_{max}\{J\} - \rho^2 - \epsilon$

To determine if Q_1 is defined positive, Sylvester's theorem is applied in (35), and it is determined that, by selecting $K_{p1}, K_{p2}, K_{d1}, K_{d2}$ such that they satisfy inequalities (30) to (33) accordingly $H_1(x_s, t)$ it will be a negative definite function.

In the analysis of $H_2(x_s, t)$ the functions are involved $\alpha_1(x_s, t)$ and $\alpha_2(x_s, t)$ as a result of the proposed Lyapunov function, that is to say

$$\alpha_1(x_s, t) = \frac{1}{2\gamma^2}[\beta\tanh(x_{s1}) + x_{s2}] \quad (36)$$

$$\alpha_2(x_s, t) = \frac{1}{2}[\gamma\ \tanh(x_{s3}) + x_{s4}] \quad (37)$$

Developing $H_2(x_s, t)$ you have to

$$H_2(x_s, t) \leq \frac{1}{4\gamma^2}\|x_{s2}\|^2 + \frac{\beta}{2\gamma^2}\|\tanh(x_{s1})\|\|x_{s2}\| + \frac{\beta^2}{4\gamma^2}\|\tanh(x_{s1})\|^2 - \frac{1}{4}\|x_{s4})\|^2 + \frac{\gamma}{2}\|\tanh(x_{s3})\|\|x_{s4}\| - \frac{\gamma^2}{4}\|\tanh(x_{s3})\|^2$$

$$H_2(x_s, t) \leq -\frac{1}{4}\begin{bmatrix} \|\tanh(x_{s1})\| \\ \|x_{s2}\| \\ \|\tanh(x_{s3})\| \\ \|x_{s4}\| \end{bmatrix}^T Q_2 \begin{bmatrix} \|\tanh(x_{s1})\| \\ \|x_{s2}\| \\ \|\tanh(x_{s3})\| \\ \|x_{s4}\| \end{bmatrix} \quad (38)$$

$$Q_2 = \begin{bmatrix} \frac{-1}{\gamma^2} & \frac{-\beta}{\gamma^2} & 0 & 0 \\ \frac{-\beta}{\gamma^2} & \frac{-\beta^2}{\gamma^2} & 0 & 0 \\ 0 & 0 & 1 & -\gamma \\ 0 & 0 & -\gamma & \gamma^2 \end{bmatrix}$$

Matrix Q_2 will be undefined for any positive constant γ and β. Finally, the inequality of Hamilton-Jacobi-Isaacs $H(x_s, t)$ it will be a negative definite function if

$$\lambda_{min}\{Q_1\} + \frac{1}{4}\lambda_{min}\{Q_2\} > 0. \quad (39)$$

1.3. Pendulum of a degree of freedom with rotational and flexible articulation

Be the mechanical system with flexible articulation defined as:

$$m\ddot{q} + g\sin(q) + K(q - \theta) = w_u \quad (40)$$
$$J\ddot{\theta} - K(q - \theta) = \tau + w_m$$

where the parameters of the plant and controller are shown in the following tables.

Description	Notation	Value	Unit
Mass of the joint	m	1.0001	Kg
Constant stiffness	K	100	Nm/rad
Moment of Inertia of the engine	J	0.02	Kg m
Moment of Inertia of the motor Gravitational constant	g	9.81	m/s

Table 1 Parameters of the pendulum of a degree of freedom
Source: Self Made

The position, the speed of the actuator and the articulation are available for the measurement at all times.

Parameters	Value
γ	7
ϵ	0.01
ρ	0.1
β	8
K_{h2}	44.7747
K'	10.791
K_g	10.791
K_{p1}	5.1
K_{p2}	3.73
K_{d1}	0.09
K_{p2}	0.18
Γ	5

Table 2 Parameters of the CGEV
Source: Self Made

The desired reference signals are defined as: $q_d(t) = \pi\sin(1.885t)$, $\theta_d(t) = q_d(t) + K^{-1}g\sin(q_d)$ and the initial condition is placed in $x(0) = \left[\frac{1}{2}\pi, 0, \frac{1}{2}\pi, 0\right]^T$, finally the system is disturbed with $w_m(t) = \pi\sin(10\pi t)$ y $w_u(t) = \pi\,cos(20\pi t)$.

ISSN: 2414- 4924

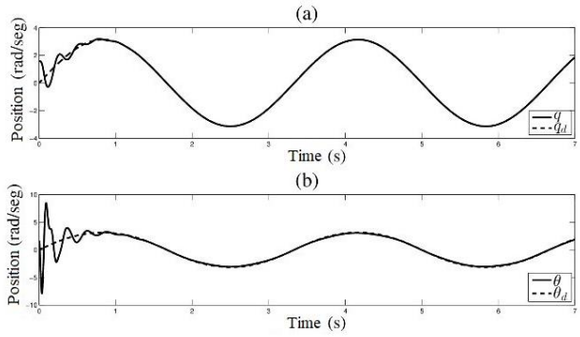

Figure 2 Performance of the system in closed loop (14) and (18), (a) Joint position and desired position, (b) Position of the actuator and position of the desired actuator
Source: Self Made

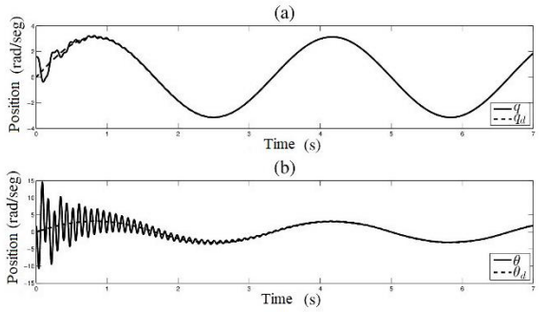

Figure 3 System performance in closed loop (14) and (18) without the non-linear control H_∞, (a) Articular position and desired position, (b) Position of the actuator and position of the desired actuator
Source: Self Made

Results

In Section I, the disturbed non-linear and time-varying plant was proposed, as well as the CGEV in which the theory is developed. Section II provides the controls that make up the CGEV in general for any system mentioned at the beginning. of the present paragraph, the controllers involved in the CGEV are the control by integral sliding mode (5) and control H_∞ non-linear (13), in section III the CGEV applied to a robot manipulator of l degrees of freedom with rotational articulations and with the elasticity effect in the presence of coupled and uncoupled perturbations, in the same way we present theorem 2 that gives solution to the non-linear H_∞ control (37) that is part of the CGEV, finally we analyze the proposed control in a pendulum of a degree of freedom with the rotational and flexible articulation and in the presence of coupled and uncoupled disturbances, the closed loop system (14) and (18) is analyzed with the help of M atLab / Simulink.

The performance of the aforementioned system is presented in figures 2 and 3, in figure 2 there is an underdamped result of the elasticity effect in the articulation and of the coupled and uncoupled disturbances to which the system was exposed, such effect and the disturbances were attenuated as time tends to infinity. Figure 3 shows a very marked underdamping in the position of the actuator, this is due to the fact that the non-linear controller H_∞ of the CGEV was eliminated, and the effects of the uncoupled perturbation take a little longer to be attenuated by the control discontinuous.

Conclusions

A variable structure global controller composed of integral sliding mode control and non-linear H_∞ control was proposed for non-linear, subacted and non-autonomous systems in the presence of coupled and uncoupled perturbations, the theory was validated with the regulation problem of movement for a robot manipulator of l degrees of freedom with rotational unions and with the effect of elasticity in each of them. In the proposed control structure, the integral sliding mode control keeps the path of the system in closed loop within the sliding mode and rejects the coupled disturbances and the control H_∞ in the sliding mode attenuates the uncoupled disturbances.

References

A. Isidori y A. Astolfi (1992), Disturbance attenuation and $\mathcal{H}_\infty$-control via measurement feedback in nonlinear systems, IEEE Transactions on Automatic Control, Vol. 37, No. 9, pp. 1283_1293.

E. Rivin (1985), Effective Rigidity of Robot Structures: Analysis and Enhancement, in proc. of the America Control Conference, 1985, Detroit, USA, pp. 381-382.

F. Castaño y L. Fridman (2006), Analysis and Design of Integral Manifolds for Systems with Unmatched Perturbations, IEEE Transactions on Automatic Control, Vol. 51, No. 5, pp. 853-858.

H. Khalil (2015), Nonlinear Control, Pearson Education, Upper Saddle River, New Jersey, ISBN: 978-0133499261.

ISSN: 2414- 4924

J. Wen y X. Jian (2001), Nonlinear Integral type Sliding surface for both Matched and Unmatched Uncertain Systems, in Proc. American Control Conference, Arlington, USA, pp. 4369-374.

L. Fridman, A. Poznyak y F. Bejarano (2014), Robust Output LQ Optimal Control via Integral Sliding Modes, New York, NY, USA: Birkhäuser, ISBN: 2324-9749.

L. Fridman, J. Barbo, F. Plestan (2016), Recent Trends in Sliding Mode Control, London, IET.

M. Rubagotti, F. Castaño, A. Ferrara y L. Fridman (2011), Integral sliding mode control for nonlinear systems with matched and unmatched perturbations, IEEE Transactions on automatic control, pp. 2699-2704, vol. 56, No. 11.

M. Spong y M. Vidyasagar (1989), Robot Dynamics and Control, New York: Wiley, ISBN: 978-0-471-61243-8.

Roger Miranda Colorado, Carlos Chavez, y Luis T. Aguilar (2017), Integral Sliding Modes with Nonlinear H∞-Control for Time-Varying Minimum-Phase Underactuated Systems with Unmatched Disturbances, Mathematical Problems in Engineering, Volume 2017, Article ID 4876019.

R. Galvan Guerra, L. Fridman (2015), Robustification of time varying linear quadratic optimal control based on output integral sliding modes, IET Control Theory and Applications, vol. 9, no. 4, pp. 563-572.

R. Kelly, V. Santibañez y A. Loria (2005), Control of Robot Manipulators in Joint Space, London: Springer Verlag, ISBN: 1439-2232.

V. Utkin (1992), Sliding Modes in Control Optimization, Berlin: Springer-Verlag, ISBN: 3-540-53516-0.

V. Utkin, J. Guldner y J. Shi (2009), Sliding Modes Control in Electromechanical Systems, second edition, Automation and control engineering series, CRC Press, ISBN: 9781420065602.

Y. Orlov y L. Aguilar (2014), Advanced $\mathcal{H}_\infty$ Control: Towards Nonsmooth Theory and Applications, New York: Birkhäuser, ISBN: 2324-9749.

ISSN: 2414- 4924

Article **ECORFAN Journal Democratic Republic of Congo**
June 2018 Vol.4 No.6 11-17

Continuous Twisting apply to a nonlinear mathematical model of sinchronous generator

Continuous Twisting aplicado al modelo matemático no lineal de un generador síncrono

RAMIREZ-YOCUPICIO, Susana†*, RUIZ-IBARRA, Joel, PALACIO-CINCO, Ramón René and RUIZ-IBARRA, Erica

Instituto Tecnológico de Sonora

ID 1st Author: *Susana, Ramirez-Yocupicio* / **ORC ID**: 0000-0001-6746-9370, **arXiv Author ID**: SusanaRamirezYoc, **CVU CONACYT ID**: 639921

ID 1st Coauthor: *Joel, Ruiz-Ibarra* / **ORC ID**: 0000-0002-4932-2006, **arXiv Author ID:** JoelRuizIbarra, **CVU CONACYT ID**: 38599

ID 2nd Coauthor: *Ramón René, Palacio-Cinco* / **ORC ID**: 0000-0002-4059-2149, arXiv Author ID: ramon.palacio, **CVU CONACYT ID**: 201437

ID 3rd Coautor: *Erica, Ruiz-Ibarra* / **CVU CONACYT ID**: 86862

Received January 18, 2018; Accepted June 20, 2018

Abstract

Electronic power systems are responsible for generating and supplying electrical power to society. It is necesary to keep suitable levels of current and voltage in order to achieve a good performance. This levels must be keep despite constant disturbances. The sinchronous generator is one device in charge of providing power to the system. In this paper we apply the Continuous Twisting Control Algorithm to provide power at a constant frequency giving robustness to the sinchronous generator robustness (insensitivity to parameter variations and disturbances and modeling errors) minimizing chattering. We take the control signal, time response and error magnitudes to verify the performance of the system. Besides, we use a normal form for the mathematical model of eigh states. Results show a correct performance of the proposed control verifying disturbances in mechanical torque and short circuit. The control signal si coninuous therefore we get a reducction of chattering.

Sincronous Generator, Twisting, Continuous Twisting

Resumen

Los sistemas electrónicos de potencia se encargan de generar y suministrar potencia eléctrica a la sociedad. Para el correcto funcionamiento de éstos sistemas, es necesario mantener niveles de voltaje y corriente estables y adecuados. Estos niveles deben cumplirse a pesar de las constantes perturbaciones a las que se encuentra sometida la red. Uno de los elementos encargados de proporcionar energía al sistema es el generador síncrono. En éste trabajo se aplica el algoritmo de control *Continuous Twisting* para garantizar una generación de potencia a frecuencia constante. Lo anterior, con el fin de proporcionar al generador la robustez característica del control por modos deslizantes (rechazo a perturbaciones acopladas al control, robustez ante cambios paramétricos y errores de modelado) minimizando el efecto *chattering*. Para lo anterior se toman en cuenta la señal de control, tiempo de respuesta y magnitudes de error. Para el diseño se utiliza una forma normal del modelo matemático no lineal de ocho estados del generador síncrono. Los resultados de simulación muestran la efectividad del control propuesto tomando en cuenta perturbaciones en el par mecánico y corto circuito. La señal de control es continua por lo tanto se obtiene una reducción de *chattering*.

Generador Síncrono, *Chattering*, Continuous Twisting

Citation: RAMIREZ-YOCUPICIO, Susana, RUIZ-IBARRA, Joel, PALACIO-CINCO, Ramón René and RUIZ-IBARRA, Erica**.** Continuous Twisting apply to a nonlinear mathematical model of sinchronous generator. ECORFAN Journal-Democratic Republic of Congo. 2018, 4-6: 11-17.

* Correspondence to Author (email: susanaramirez64@gmail.com)
† Researcher contributing first author.

I. Introduction

Much of the electricity generation is carried out by means of synchronous generators (Del Toro, 1992). These generators, with the aid of other devices such as photovoltaic panels, maintain a delicate balance between the generation and demand of electrical energy (Kundor, 1994). To achieve the above, it requires adequate operating margins, mainly in frequency and voltage. This has been achieved with the help of different control techniques applied to the synchronous generator.

For the control of the generator in an electrical network, the aid of linearisations has traditionally been used. These make decision making easier. However, when using simple control schemes, important dynamic characteristics are no longer considered (Kothari, 2008). To compensate for this loss of information, the operating margins of the generator are reduced. That is to say, due to the uncertainty, in the event of disturbances or critical variations in the demand for energy, it is decided to disable the operation of the generator. In such a way that, as a consequence, a considerable reduction in the robustness and capacity of the network is obtained.

Due to the above, the development of controllers applied to the synchronous generator has aroused the interest of many researchers. As a result, new control techniques have been obtained and applied, among them the direct method of Lyapunov (Machowski, 2000), linear techniques for feedback (Gao, 1992, Kazemi, 2007), diffuse control (Hiyama, 1997), neural networks (Shamsollahi, 1997), passivity (Xi, 2000), analysis of energy functions (Shen, 2005) and adaptive control (Rintoja, 2000). In addition to the previous methods, there is control by classic sliding modes (Huerta, 2009, Soto-Cota, 2006, Loukianov, 2011) which, due to their nature, in addition to presenting adequate levels of frequency and voltage, provides robustness against disturbances and parametric changes (Shtessel et al., 2014; Drazenovic, 1969).

A disadvantage of the application of sliding modes is that the first generations of these techniques, because the control signal is discontinuous at high frequency, present chattering (Slotine, 1983).

This effect causes low performance in the controller, high energy losses due to heat in electrical circuits and physical wear caused by mechanical movement (Utkin, 1993). Chatterign is one of the main reasons why new sliding control techniques have been developed (Levant, 1993).

One of the first techniques to reduce chattering is the application of a second-order or higher-order sliding mode algorithm (Shtessel, 1998). The first of this type is the second order Twisting (Shtessel, 2014), followed by Super-Twisting (Kamal, 2014) and Continuous Twisting (Torres Gonzales, 2016).

Each one with significant improvements in the control signal. In such a way that it is reduced, and in some cases, chattering is eliminated (Boiko, 2005). The Continuous Twisting control algorithm, in addition to providing a continuous control signal, compensates for disturbances, in such a way that it provides robustness to the system, in addition to ensuring convergence in finite time to the sliding surface and to its first and second derivatives..

The objective of this article is the application of a Continuous Twisting control to a synchronous generator to provide robustness against perturbations and unmodeled dynamics, decreasing the chattering effect resulting from the first generations of sliding modes. The above, in order to make improvements in the electric generation process, increasing the operating margins of the synchronous generator and guaranteeing the quality of frequency and voltage in adverse situations.

This article is structured as follows. Section II presents the mathematical model of the synchronous generator. In Section III, the control objective is clearly defined. In section IV a first control structure is proposed. In Section VI Continuous Twisting is applied through simulations, taking into account disturbances in the mechanical torque, parametric changes and short circuit. Finally, in section VI, the conclusions of the article are presented.

ISSN: 2414- 4924

II. Mathematical model of the synchronous generator

This paper uses a non-linear mathematical model of eight states:

$$x = [x_1, x_2, x_3, x_4, x_5, x_6, x_7, x_8]$$

where x_1 is the loading angle, x_2 is the angular velocity, x_3 is the flow link of the field winding, x_4, x_5 and x_6 are the flow link of the damping windings and finally x_7 and x_8 represent the stator currents in the direct axis and quadrature respectively (Soto, 2000). The mathematical model (Soto-Cota, 2006) is shown below:

$$\begin{aligned}
\dot{x}_1 &= x_2 - w_b \\
\dot{x}_2 &= \tfrac{w_b}{2H}(T_m - T_e) \\
\dot{x}_3 &= b_1 x_7 + b_2 x_5 + b_3 x_3 + w_b V_f \\
\dot{x}_4 &= c_1 x_8 + c_2 x_6 + c_3 x_4 \\
\dot{x}_5 &= d_1 x_7 + d_2 x_3 + d_3 x_5 \\
\dot{x}_6 &= e_1 x_8 + e_2 x_4 + e_3 x_6 \\
\dot{x}_7 &= h_1 V_d + h_2 V_f + h_3 x_7 + h_4 x_3 + h_5 x_5 + \\
&\quad h_6 x_2 x_4 + h_7 x_2 x_6 + h_8 x_2 x_8 \\
\dot{x}_8 &= k_1 V_q + k_2 x_8 + k_3 x_4 + k_4 x_6 + k_5 x_2 x_3 + \\
&\quad k_6 x_2 x_5 + k_7 x_2 x_7
\end{aligned} \tag{1}$$

where w_b is the desired angular velocity, T_m is the mechanical torque, $T_e = a_1 x_3 x_8 + a_2 x_5 x_8 + a_3 x_4 x_7 + a_4 x_6 x_7 + a_5 x_7 x_8$ is the electromagnetic pair, $V_d = V \sin x_1$, $V_q = V \cos x_1$ and V represents the bus to which the generator is connected. V_f, which is generally a constant value in the order of the millivolts (Huerta, 2008), in this work it is considered as the control input, ie $V_f = u$.

The rest of the values represent parameters of the synchronous generator and are described in Annex 1.

III. Control objective

The control objective is to keep the synchronous generator providing power at a frequency of 60Hz. For this, it is necessary that the rotor rotate at synchronous speed w_b. The above, taking into account the stability of the voltage at the generator terminals. Therefore, an error function is defined $e = x_2 - w_b$ and it is taken as the sliding surface and its derivative is obtained,

$$s = s_1 = e = \dot{x}_1 = x_2 - w_b \tag{2}$$

$$\dot{s}_1 = s_2 = \dot{x}_2 = \tfrac{w_b}{2H}(T_m - T_e). \tag{3}$$

In this way, when the error is equal to zero $x_2 = w_b$.

IV. First control structure

It defines $q_1 = b_1 x_7 + b_2 x_5 + b_3 x_3$ and $\dot{x}_3$ is taken into account as the control channel from (1). The following control structure is proposed:

$$u = \tfrac{1}{w_b}(-q_1 + v_1) \tag{4}$$

where v_1 is the new control to be defined. In this way, replacing (4) in (1), $\dot{x}_3$ is defined as follows

$$\dot{x}_3 = v_1. \tag{5}$$

Calculating in $\dot{s}_2$, and taking into account (4), (5) and $\dot{x}_7$, that also presents the control signal explicitly, you get

$$\begin{aligned}
\dot{s}_2 = -\tfrac{w_b}{2H}\{(w_b a_1 x_8 + h_2 q_3)\left[\tfrac{1}{w_b}(-q_2 - \right. \\
\left. v_1)\right] + a_1 x_8 q_1 + q_2 + q_3 q_4\}
\end{aligned} \tag{6}$$

where

$$\begin{aligned}
q_2 &= a_3 \dot{x}_4 x_7 + a_2 \dot{x}_5 x_8 + a_4 \dot{x}_6 x_7 + \\
&\dot{x}_7(a_3 x_4 + a_4 x_6 + a_5 x_8) + \dot{x}_8(a_1 x_3 + \\
&a_2 x_5 + a_5 x_7)
\end{aligned}$$

$$q_3 = a_3 x_4 + a_4 x_6 + a_5 x_8$$

$$\begin{aligned}
q_4 &= h_1 V_d + h_3 x_7 + h_4 x_3 + h_5 x_5 + h_6 x_2 x_4 + \\
&\quad h_7 x_2 x_6 + h_8 x_2 x_8.
\end{aligned}$$

Defining v_1 as follows

$$v_1 = -\left(\frac{2H}{w_b a_1 x_8 + h_2 q_3}\right) v. \tag{7}$$

Substituting (7) in (6) and taking into account (3) you get the following

$$\begin{aligned}
\dot{s}_1 &= s_2 \\
\dot{s}_2 &= v + q_5
\end{aligned} \tag{8}$$

where

$$q_5 = \tfrac{h_2}{2H} q_1 q_3 - \tfrac{w_b}{2H}(q_2 + q_3 q_4).$$

The control by sliding modes will be carried out taking into account (8). Being v the new control signal to be designed and it is assumed that $|\dot{q}_5| \leq q \in \mathbb{R}$.

V. Application of the Continuous Twisting control algorithm

To use this control algorithm surface information is required s_1 and its first derivative s_2, which, in turn, are equal to (2) and (3) respectively.

The control algorithm v has the following form:

$$v = -K_1\lceil z_1\rfloor^{\frac{1}{3}} - K_2\lceil z_2\rfloor^{\frac{1}{2}} + \eta \qquad (10)$$
$$\dot{\eta} = -K_3\lceil z_1\rfloor^{0} - K_4\lceil z_2\rfloor^{0}$$

considering the nomenclature $\lceil w\rfloor^{p} = |s_j|^{p}\text{sign}(s_j), j = \{1,2\}$ y $p = \left\{1, \frac{1}{3}, \frac{1}{2}\right\}$.

The values of the gains were obtained assuming q = 3.011503. Earnings are adjusted according to (Torres Gonzales, 2016).

Which suggests that

$$K_1 = 1.109878\, L^{\frac{2}{3}}$$
$$K_2 = 1.341066\, L^{\frac{1}{2}}$$
$$K_3 = 0.033206\, L$$
$$K_4 = 0.016846\, L$$

Where L is given by the equation Lq = 0.002. Therefore L = 1505.751973. So the gains are like

$$K_1 = 145.8067188$$
$$K_2 = 40.127493$$
$$K_3 = 50$$
$$K_4 = 25.36589774.$$

This structure is stable and presents convergence to zero s_1 and s_2 in finite time. It also presents insensitivity to disturbances buffered to control. It should be mentioned that the control signal v is continuous.

VI. Simulation results of the controlled system with disturbances

To obtain the simulation results, the nominal parameters of a three-phase synchronous generator of 555 MVA are used, with 24 kV at a frequency of 60 Hz. The rotor has two poles, three phases and is considered an infinite bus. The parameters of the synchronous generated and the external network in values in per unit (Huerta, 2009). Figure 1 shows the external network of a synchronous generator connected to an infused bus. Inductance and line resistance are considered.

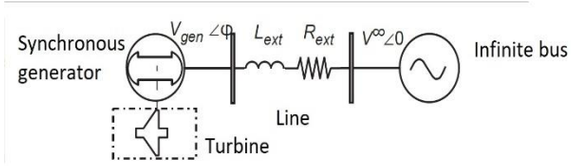

Figure 1 Synchronous generator connected to an infinite bus
(Soto-Cota, 2006)

To check the control of the plant in closed loop with the controller, it was subjected to perturbations in the electromechanical pair, short circuit and parametric changes. An increase in the mechanical torque of 0.2 pu was applied from the time t = 3 sec to the time t = 3.5 sec.

Parametric changes were made t = 6 sec at t = 6.5 sec, a change of 10% was introduced in the values b_2 and h_4, both in the control channel. The short circuit was applied for 0.1 sec, starting at t = 10 sec, to achieve this, the infinite bus voltage was brought to $V_{inf} = 0.7$ pu.

The results of the angular velocity (control objective), the electromechanical torque, the control signal and the voltage at the generator terminals are shown below. The values of the initial conditions are presented in Annex 2.

In graphic 1, the angular velocity shows convergence in finite time. This is to be expected because the sliding surface is designed so that the angular velocity is the synchronous speed.

ISSN: 2414- 4924

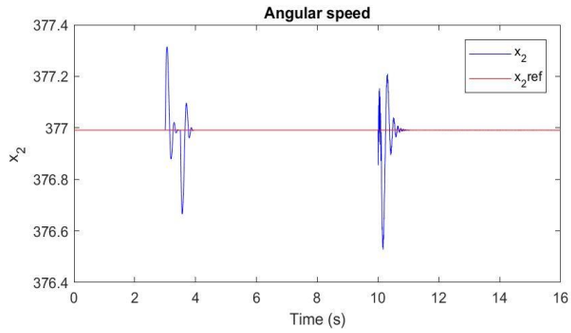

Graphic 1 Angular velocity
Source: Self Made

The important to note that parametric changes do not affect the control objective, the angular velocity. Graphic 2 shows how the electromechanical pair follows the electromagnetic torque despite being disturbed. Finite time convergence is also shown because it has a very close relationship with the first derivative of the sliding surface. In this graph it is possible to observe a small perturbation in the electromechanical pair during the parametric changes.

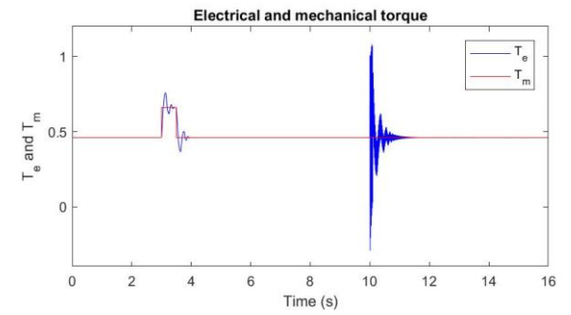

Graphic 2 Electromechanical torque and electromagnetic torque
Source: Self Made

Graphic 3 shows Voltage in terminals and the infinite bus voltage. The disturbance in the mechanical torque does not affect it much, however, the perturbation of the short circuit is more significant.

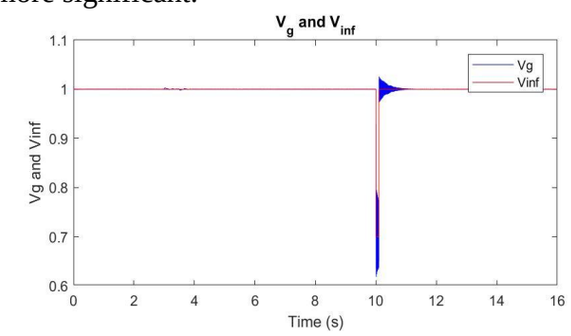

Graphic 3 Voltage in terminals and infinite bus voltage
Source: Self Made

The generated control signal can be seen in graphic 4, a continuous control signal is obtained as a result. Parametric changes generate a change in the control signal. The first is at the moment of detecting the change of the parameter with error of 10% and the second is to return to normal.

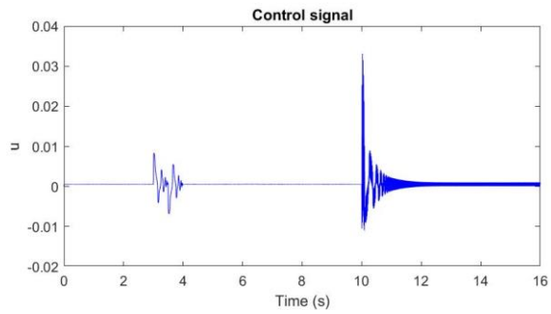

Graphic 4 Control signal
Source: Self Made

Graphic 5 shows the convergence to zero at the time of the sliding surface. In blue the surface is appreciated and in red the value zero. Note that the sliding surface is not affected by the parametric changes. This is because the disturbances were made on the control channel.

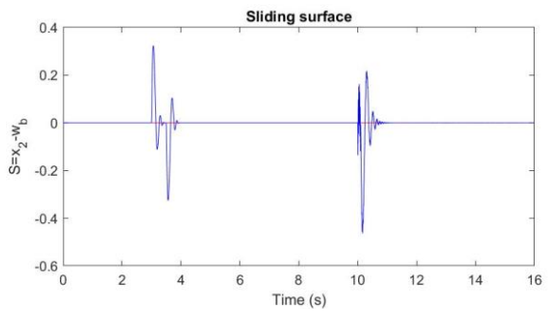

Graphic 5 Sliding surface
Source: Self Made

The derivative of the sliding surface is shown in graphic 6.

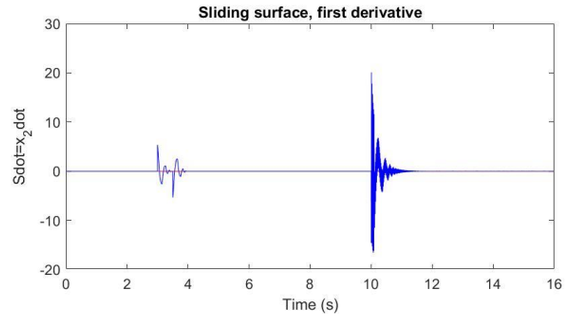

Graphic 6 Derived from the sliding surface
Source: Self Made

The derivative of the sliding surface, like the surface, has finite time convergence. In blue the surface is appreciated and in red the value zero. Note that the sliding surface is not affected by the parametric changes.

VII. Conclusions

The present work shows the application of a Continuous Twisting control algorithm with the help of a first proposed control structure. The resulting control signal is continuous therefore a chattering elimination is obtained. Unlike other algorithms by sliding modes that, due to the discontinuous nature of the resulting control signal, generate chattering.

The gains proposed in this work guarantee the stability of the system as long as the present conditions are met. The use of the first control structure can be applied to other algorithms such as Twisting and Super-Twisting, facilitating the comparison between them. For future work, it is recommended that an observer be used to estimate difficult-to-measure states and, thus, get closer to an implementation.

References

Bialek, S., Bumby, J. W., AbiSamra, J. R., Machowski, N. & Robak, J. (2000). Decentralised stabilityenhancing control of synchronous generator. *IEEE Transactions of Power Systems*, *15*, 1336-1344.

Boiko, I. & Fridman, L. (2005). Analysis of chattering in continuous sliding mode controllers. *IEEE Transactions on Automatic Control, 50*, 1442-1446.

Del Toro, V. (1992). *Electric Power Systems.*, New Yersey, NY, E.U.: Prentice Hall.

Drazenovic, B. (1969). The invariance condition in variable structure systems. *Automática, 5*, 287-295.

Gao, L., Chen, Y., Fan & DFL, H. Ma. (1992) Nonlinear design with applications in power systems. *Automatica, 28*, 975-979.

Hiyama, T., Ueki T. & Andou, A. (1997) Integrated fuzzy logic generator controller for stability enhancemet. *IEEE Transactions Energy Conversion, 12*, 400-406.

Huerta, H., Loukianov, A. & Cañedo, J. M. (2008). *Integral Sliding Modes with Block Control of Multimachine Electric Power System.* SystemsStructure and Control, Petr Husek.

Huerta, H., Loukianov, A. & Cañedo, J. M. (2009). Multimachine power system control: integral SM approach. *IEEE Transactions on industrial electronics, 56*, 2229 - 2236.

Kamal, S., Chalanga, A., Moreno, J. A., Fridman, L. & Bandyopadhyay. (2014). High order super twisting algorithm. *IEEE Workshop on Variable Structure Systems*, 14.

Kazemi, A., Jahed, M. R. & Naghshbandy, A. H. (2007). Application of a new multi variable feedbach linealization method for improvement of power systems transient stability. *International Journal Electronic Power Energy Systems, 29*, 322-328.

Kothari, I. J. & Nagrath, I. J. (1994). *Sistemas eléctricos de potencia.* California, E. U.: McGrawHill.

Kundor, P. (1994). *Power systems stability and control*. California, E. U.: McGrawHill.

Levant, A. (1993). Sliding order and sliding accuracy in sliding mode control. *International Journal control, 58*, 1247-1263.

Loukianov, A. G., Cañedo, J. M., Fridman, L. M. & Soto-Cota, A. (2011). Hight Order Block Sliding Mode Controller for a synchronous generator with an exciter system. *IEEE Transactions on industrial electronics, 58*, 337-347.

Rintoja, J. (2000). *Modern power system stabilizer approaches.* Mamburgo, Eslovenia: University of Maribor, Faculty of electrical engineering and computer science, 2000.

Shamsollahi, P. & Malik, O. P. (1997). An adaptive power system stabilizer using on-line trained neuronal network. *IEEE Transactions Energy Convers, 12*, 382-387.

Shen, T., Sun, R., Ortega, R. & Mei, S. (2005). Energy-shaping control of synchronous generator with exciter-governor dual control-loops. *International Journal Control, 78*, 100-111.

ISSN: 2414- 4924

Shtessel, Y., Edwards, C., Fridman, L. & Levant, A. (2014). *Sliding Mode Control and Observation.*, New York, NY, E.U.: Control Engineering, Borkhauser

Shtessel, Y. B. & Buffington, J. M. (1998). Continuous sliding mode control. Proccedings of the 1998, *American Control Conference*. Filadelfia, Pensilvania.

Slotine, J. J. & Sastry, S. S. (1983). Tracking control of non-linear systems using sliding surfaces with application to robot manipulators. *International Journal Control, 38*, 465-492.

Soto, A. (2000) *Control robusto de sistemas no lineales por modos deslizantes aplicación y control de un generador síncrono.* Cinvestav, Guadalajara, México.

Soto-Cota, A., Fridman, L. M., Loukianov, A. G., & Cañedo, J. M. (2006). Variable structure control of synchronous generator singularly perturbed analysis. *International Journal of Control, 79*, 1-13.

Torres Gonzales, V., Fridman, L. & Morenoi, J. A. (2015). Continuous twisting algorithm. *2015 54 IEEE Conference on Design and Control*.

Utkin, V. (1992). *Sliding Mode Control and Optimization.* E.U.: Springer Verlag.

Xi, Z. & Cheng, D. (2000). Passivity based stabilization and h infinity control of the hamiltonian control systems with dissipation an its applications to power systems. *International Journal Control, 73*,1686-1691.

Annex 1

The parameters of the synchronous generator obtained from the specifications given in the article are:

$w_b = 376.911$ $H = 7.05$
$T_m = 0.4610$ $V_f = 5.5305 \times 10^{-4}$
$a_1 = 0.6495$ $a_2 = 0.2$
$a_3 = -0.2628$ $a_4 = -0.5714$
$a_5 = 0.02$ $b_1 = -0.186$
$b_2 = 0.1329$ $b_3 = -0.2329$
$c_1 = -0.7757$ $c_2 = 1.4776$
$c_3 = -1.9061$ $d_1 = -11.6667$
$d_2 = 27.0609$ $d_3 = -33.3333$
$e_1 = -10$ $e_2 = 8.7609$
$e_3 = -14.2857$ $h_1 = -876.7235$
$h_2 = 569.3989$ $h_3 = -9.2142$
$h_4 = 12.2348$ $h_5 = -15.3032$
$h_6 = -0.6112$ $h_7 = -1.3289$
$k_1 = -837.758$ $k_2 = -16.5025$
$k_3 = 10.0116$ $k_4 = -17.2776$
$k_5 = 1.4432$ $k_6 = 0.4444$
$k_7 = -0.9556$ $V_{inf} = 1$
$V_d = V_{inf}\sin(x_1)$ $V_q = V_{inf}\cos(x_1)$.

Annex 2

The initial conditions calculated are:

$x_1 = 0.7565$ $x_2 = 376.9911$
$x_3 = 1.0815$ $x_4 = -0.635$
$x_5 = 0.7734$ $x_6 = -0.635$
$x_7 = 0.2988$ $x_8 = 0.3508.$

ISSN: 2414- 4924

Article **ECORFAN Journal Democratic Republic of Congo**
June 2018 Vol.4 No.6 18-28

Development of an application for monitoring the level of a fluid, using a cell phone, Bluetooth communication and Arduino platform

Desarrollo de una aplicación para el monitoreo del nivel de un fluido, utilizando un teléfono celular, comunicación Bluetooth y plataforma Arduino

GUTIERREZ-GRANADOS, Cuitláhuac*†, ESPINOSA-AHUMADA, Elias and HERNÁNDEZ-TOVAR, Jonathan

Universidad Tecnológica de San Juan del Río, Carrera de Mecatrónica, Av. La Palma No. 125, Col. Vista Hermosa, San Juan del Río, Querétaro 76800, México

ID 1st Author: *Cuitláhuac, Gutierrez Granados* / **ORC ID**: 0000-0003-1711-6335, **Researcher ID Thomson**: R-9602-2018, **CVU CONACYT-ID**: 288644

ID 1st Coauthor: *Elias, Espinosa Ahumada* / **ORC ID**: 0000-0001-5860-2774, **Researcher ID Thomson**: S-1344-2018, **CVU CONACYT-ID**: 288636

ID 2nd Coauthor: *Jonathan, Hernández Tovar* / **ORC ID**: 0000-0002-6473-0809, **Researcher ID Thomson**: S-1319-2018, **CVU CONACYT-ID**: 946114

Received January 18, 2018; Accepted June 20, 2018

Abstract

The measurements of fluid height level in different situations such as in cisterns, tanks or wastewater tanks, are important but involve difficulties and precautions taken by the user to avoid possible falls or inhale toxic vapors; the present project has the purpose of measuring the height level of the fluid using an ultrasonic sensor, also integrating the Arduino Mega platform as an information processing and monitoring system, as well as a Bluetooth wireless communication circuit, in order to transmit the information obtained to a smartphone type cell phone, agile safe and reliable. The tangible benefits of the project, in addition to the security it will offer the user, are the economic ones, based on low cost components compared to the products of industrial brands. Finally, this project can be integrated as part of others related to renewable energies and industrial processes, which require measurements of the level of various liquids.

Arduino Mega, Bluetooth, Ultrasonic

Resumen

Las mediciones de nivel de altura de fluidos en situaciones diversas como son en las cisternas, tanques o depósitos de aguas residuales, son importantes pero conllevan dificultades y toma de precauciones por parte del usuario para evitar posibles caídas o aspirar vapores tóxicos; el presente proyecto tiene la finalidad de medir el nivel de altura del fluido utilizando un sensor ultrasónico, integrando también la plataforma Arduino Mega como sistema de procesamiento de información y monitoreo, así como un circuito de comunicación inalámbrica Bluetooth, para poder transmitir la información obtenida a un celular tipo Smartphone de manera, ágil segura y confiable. Los beneficios tangibles del proyecto además de la seguridad que ofrecerá al usuario, son el económico al basarse en componentes de bajo costo, este proyecto puede integrarse como parte de otros relacionados con las energías renovables y los procesos industriales, que requieren mediciones del nivel de diversos líquidos.

Arduino Mega, Bluetooth, Ultrasónico

Citation: GUTIERREZ-GRANADOS, Cuitláhuac, ESPINOSA-AHUMADA, Elias and HERNÁNDEZ-TOVAR, Jonathan. Development of an application for monitoring the level of a fluid, using a cell phone, Bluetooth communication and Arduino platform. ECORFAN Journal-Democratic Republic of Congo. 2018, 4-6: 18-28.

* Correspondence to Author (email: cgutierrezg@utsjr.edu.mx)
† Researcher contributing first author.

Introduction

The measurement of one variable and consequently the calculation of others is important in many industrial processes, which is why it is proposed in the present project the quantification of the height of the level of a fluid, in this case water contained in an exprofeso container for it and from this quantification calculate the volume of liquid and the percentage of filling with respect to the maximum capacity considered.

The measurement of the height of the fluid level will be made using a low cost ultrasonic sensor, an Arduino Mega card as a control platform, a Bluetooth module for wireless communication and an application app designed, created and installed on a Smartphone type phone and so on to have a remote monitoring of the three important variables to know: height of the fluid level, volume and percentage of filling.

Objective

Development of a low cost experimental prototype that allows the measurement of the height of a water level, calculating additionally the volume of the fluid and the filling percentage; these variables being monitored remotely with a smartphone via a Bluetooth link.

Development

Materials and characteristics

Below is a list and brief description of the materials to be used in this project.

1 Ultrasonic sensor HC-SR04, integrated in a PCB with four terminals to connect, this will be powered and connected by means of the Arduino Mega Card

The HC-SR04 sensor is an excellent choice as an ultrasonic distance sensor. Its cost / benefit ratio makes it optimal for a wide range of applications. The use of this module is quite simple because all the control, transmission and reception electronics are contained in a PCB. The user should only send a trigger pulse and measure the time at high of the response pulse. Only 4 wires are required to complete the interface with the **HC-SR04** sensor module.

The **HC-SR04** is compatible with most microcontrollers on the market, including the Arduino UNO, Arduino MEGA and other compatible cards that work with 5 volts. There are libraries for this module that make the part of the software is solved in a very simple way.

Main features of the HC-SR04 Ultrasonic distance sensor:

- 5 volts power
- Simple interface: Only 4-wire Vcc, Trigger, Echo, GND
- Measuring range: 2 cm to 400 cm
- Supply current: 15 mA
- Pulse frequency: 40 KHz
- Ultrasonic pulse opening: 15º
- Trigger signal: 10 µs
- Dimensions of the module: 45x20x15 mm.

(GEEK FACTORY, s.f.)

Figure 1 Ultrasonic sensor HC-SR04 Top view
Source: www.google.com

Figure 2 Ultrasonic sensor HC-SR04 Bottom view
Source: www.google.com

ISSN: 2414- 4924

1 Arduino Mega Card, is an open-source development card built with an Atmega2560 microcontroller that has input and output (I / O), analog and digital pins. This card is programmed in a development environment that implements the Processing / Wiring language. Arduino can be used in the development of autonomous interactive objects or can communicate to a PC through the serial port (conversion with USB) using languages such as Flash, Processing, MaxMSP, etc. The possibilities of carrying out Arduino-based developments are limited to the imagination. The Arduino Mega has 54 digital input / output pins (14 of which can be used as PWM outputs), 16 analog inputs, 4 UARTs (serial hardware ports), 16MHz crystal oscillator, USB connection, power jack, connector ICSP and reset button. Arduino Mega incorporates everything necessary for the microcontroller to work; simply connect it to your PC by means of a USB cable or an external power supply (9 up to 12VDC). The Arduino Mega is compatible with most of the shields designed for Arduino Duemilanove, diecimila or UNO.
(Chile), s.f.).

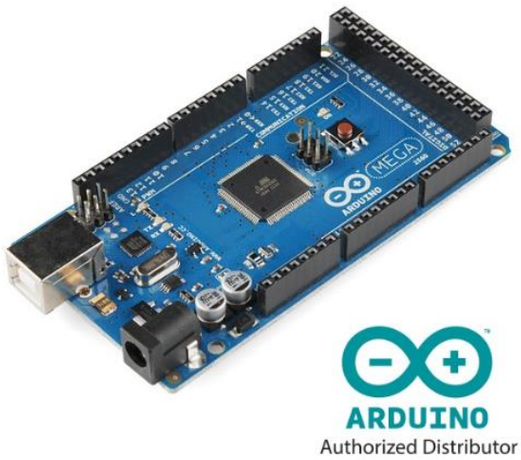

Figure 3 Arduino Mega
Source: www.google.com

1 **Bluetooth module HC-05,** which will allow communication between the Arduino Mega card and the resident app on a Smartphone-type phone, via Bluetooth. The module of Bluetooth HC-05 is the one that offers a better ratio of price and characteristics, since it is a Master-Slave module, it means that in addition to receiving connections from a PC or Tablet, it is also capable of generating connections to other devices Bluetooth This allows us, for example, to connect two Bluetooth modules and form a point-to-point connection to transmit data between two microcontrollers or devices.

(GEEK FACTORY, s.f.)

Figure 4 Módulo HC05
Source: www.google.com

1 **LCD display 16x2 model LMG-16D2T,** which will allow an information display locally, specifically: height of the fluid level and the calculated volume thereof.

Figure 5 Display LCD 16x2
Source: www.google.com

1 **Unicel sphere** 4 cm in diameter, used as a float (option 1) and lined with aluminum foil.

1 **Cylindrical cork disk** of 4 cm diameter by 2 mm thickness, also used as a float (option 2), this is aluminum foil lining.

1 **PVC tube** with an approximate length of 40 cm and an inside diameter of 2 inches. The aforementioned tube will contain the float inside and at one end it will have placed the ultrasonic sensor.

ISSN: 2414- 4924

1 **Cylindrical plastic container** of approximately 19 liters capacity, this container will serve as a water container.

1 **Phone type Smartphone** where the application will be created and installed, to establish communication with the level measurement system and receive information to be monitored in real time.

1 **Power supply** 12 VDC / 2 A, to power the Arduino Mega card, which in turn will provide power to the ultrasonic sensor, Bluetooth module and LCD Display.

1 **Small water pump,** which will serve to fill or drain the water in the plastic cylindrical bucket.

Theory

Ultrasound sensors are very useful for measuring distances and detecting obstacles.

The operation is simple, it sends an inaudible ultrasonic signal and gives us the time it takes to go back and forth to the nearest obstacle that it detected.

Generally they are formed by two cylinders placed side by side, one of them is the one that emits the ultrasonic signal, while the other is the one who receives it, it is a very simple system but it does not stop being effective.

The HC-SR04 sensor in particular has a very good sensitivity of the order of 3 mm, taking into account that most of the applications where this sensor is used is to measure or detect obstacles or distances greater than several centimeters, we can say that its sensitivity is very good.

The HC-SR04 sensor counts the time that elapses between the emission and the reception of the ultrasonic signal, clearly we can deduce that the time is dependent on the distance, the signal will take longer to go and return if the object is far away than if it is close.

Recalling some basic physics equations we know that **d=v*t** (the distance traveled is equal to the speed of the object in motion for the time it takes to arrive).

We have the time, but what is the speed of the signal? To answer that question we have to be clear that the sensor emits an ultrasonic signal and it travels at the speed of sound, at approximately 340 m / s (meters / second). If, for example, the HC-SR04 sensor gives us a reading of 1,003 ms (milliseconds) and we apply the above formula, we have left;

$$d = 340\frac{m}{s} * 1.003\, ms = 0.341m \qquad (1)$$

meters, but since this time is the round trip, the real distance to the object will be half, that's why we divide the result between two, which gives us a final result of 0.170 meters (ie 17 cm or 170 mm).

Obviously the sensor alone is not much use, we need a microcontroller to read the data that gives us and perform the relevant calculations, if what we want to develop is practical, no doubt that the best option we can choose is the Arduino platform.
(etools, 2018)

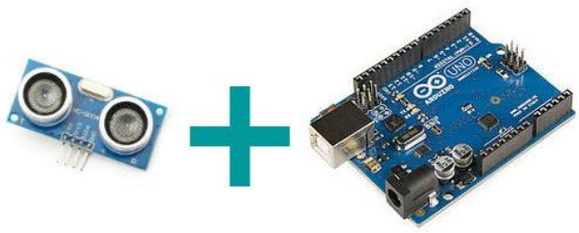

Figure 6 Ultrasonic Sensor + Arduino
Source: www.google.com

Physical Implementation

First, it was conceptualized that the measurement of the height of the water level of a fluid (specifically in this case clean water "from the tap"), would be made by measuring the distance of the float contained inside a PVC tube with respect to the sensor ultrasonic placed on one end of the tube, knowing this distance you could calculate the height of the water column. For this it is important to mention that they were tested as a float - where the ultrasonic wave bounces off - both an aluminum-lined unicel sphere and a cork disk also lined with aluminum, both have excellent buoyancy.

ISSN: 2414- 4924

Based on various tests, the convenience of opting for the aluminum-lined cork float was determined; the attributes in its favor were that it protruded less from the surface of the water compared to the sphere that practically its 4 cm in diameter were out of the water, which increased the height offset measured by the ultrasonic sensor, furthermore its curvature leads to less accurate measurements of the echo time of the sonic signal. The ultrasonic sensor-float set of PVC cork-pipe was fixed vertically to the interior of the 19-liter plastic bucket. Taking advantage of the fact that the liquids maintain the same level due to the "property of communicating vessels", that is, the water level will be the same outside that inside the PVC pipe, as long as it has perforations that allow water to be evenly distributed. . These perforations are in the lower side of the PVC pipe.

"Communicating vessels" is the name given to a set of containers communicated by its lower, upper or lateral part and that contain a homogeneous liquid; it is observed that when the liquid is at rest it reaches the same level in all the containers, without influencing the shape and volume of these. When we add a certain amount of additional liquid, it moves to a new equilibrium level, the same in all containers. The same happens when we tilt the glasses; although the position of the vessels changes, the liquid always reaches the same level. This is because the atmospheric pressure and gravity are constant in each vessel, therefore, the hydrostatic pressure at a given depth is always the same, without influencing its geometry or the type of liquid. Blaise Pascal demonstrated in the seventeenth century, the pressure exerted on a mole of a liquid, is transmitted in its entirety and with the same intensity in all directions (Pascal's Principle). "
(Wikipedia enciclopedia libre, s.f.)

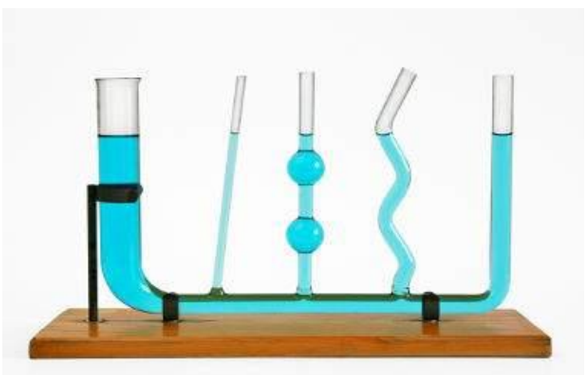

Figure 7 Communicating vessels
Source: www.google.com

The ultrasonic sensor was properly fixed on the top of the PVC tube, keeping a safe distance from the maximum water level of the cuvette, this distance is approximately 15 cm. Electrical cables were added as a means of connection of the ultrasonic sensor with the Arduino Mega card and thus power the first voltage and receive and send the signals to be processed to quantify the proximity distance of the float with respect to the ultrasonic sensor.

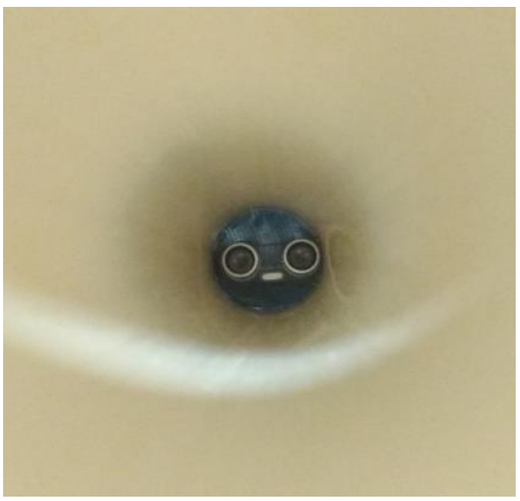

Figure 8 View inside the PVC tube where the ultrasonic sensor was placed
Source: Own Elaboration

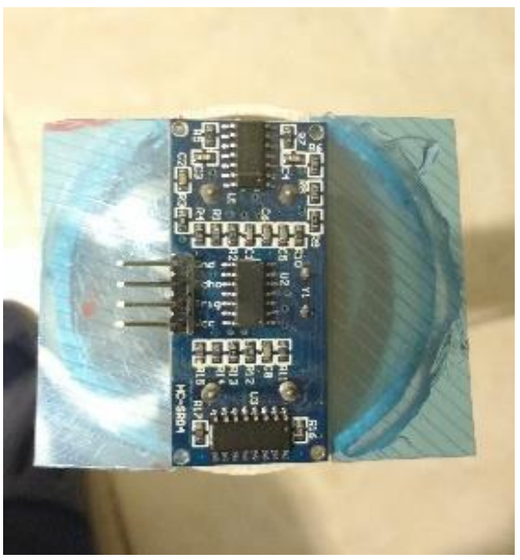

Figure 9 Ultrasonic sensor placed on one end of the PVC pipe
Source: Own Elaboration

ISSN: 2414- 4924

Figure 10 PVC tube assembly, ultrasonic sensor with cables and aluminum-lined unicel sphere.
Source: Own Elaboration

Figure 11 Disc type float, aluminum lined cork material placed in the PVC pipe
Source: Own Elaboration

The Arduino Mega card is the core element of control, it energizes and receives the signals from the ultrasonic sensor and with the appropriate program and relevant calculations the float distance is determined, from this and other data such as maximum water level height, radius of the container bucket; You can process and calculate variables to be monitored, such as: height of the fluid level, fluid volume and percentage of filling of the cuvette. These variables are issued as digital information via Bluetooth wireless communication using the HC-05 module, which will establish communication with a Smartphone-type telephone using an application specifically designed for it.

It is worth mentioning that a 16x2 LCD display is also connected to the Arduino Mega to locally visualize the variables of fluid level height and fluid volume. This connection of the LCD involves the electrical energization of the same, the control signals, data signals and contrast control on the screen. The aforementioned parts are for the moment exposed for experimentation, thinking that in a later development they can be contained in a hermetic cabinet for their protection.

Figure 12 Integration of the elements for the water level measurement system contained in the bucket
Source: Own Elaboration

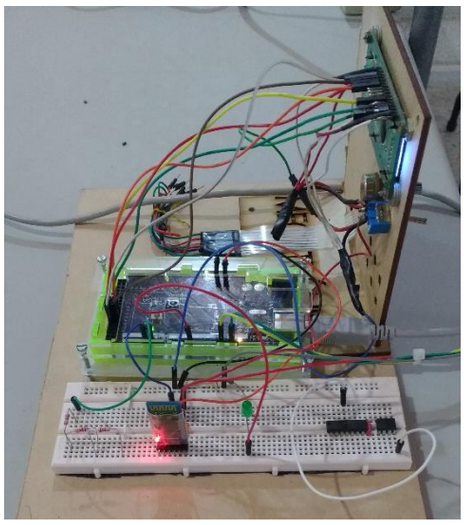

Figure 13 System composed of LCD display, Arduino Mega and Module HC-05
Source: Own Elaboration

ISSN: 2414- 4924

Arduino programming

A conceptual and general description of the program generated in the IDE environment of development, edition and compilation of Arduino is the one described below:

Calling libraries to support the program, specifically the management of the LCD display.

Declaration and types of variables to be used.

A void setup () function, where the required inputs and outputs are configured, the LCD display is initialized and initialization of the serial ports.

A void radar function (), where you have the instructions to use the HC-SR04 ultrasonic sensor, obtain the response time of the sonic echo, calculate the distance of the float placed inside the PVC tube and other calculations to determine height the water level, fluid volume and filling percentage; considering the appropriate adjustments in the equations.

A void monitor () function, where information is displayed on the personal computer on the serial monitor of the Arduino development environment.

A void function displays_LCD (), where you have instructions to display the information on the LCD display.

A void function communicates (), where you have the instructions to establish bidirectional communication with the Bluetooth module HC-05 and display the information on the smartphone, which has an app application edited for this purpose.

A main and cyclic function void loop (), where the previous functions are called for execution as subroutines.

```
28
29 float altura_max=25.25; // altura máxima de la columna de agua en cm, equivalente a 15 litros en l
30 float radio= 14.4; // radio en cm de la cubeta cilindrica
31 float pi=3.14; //constante matematica
32 float diametro_esfera= 3.6; // esfera flotador en cm que detecta el sensor ultrasonico
33 float factor_correcion=14.5;//factor de correcion para altura en cm
34
35 char caracter=' ';
36
37 void setup() {
50
59 void loop()  //programa principal ciclico
60 {
67
68 void comunica ()
69 {
97
98 void radar() //rutina para utilizar el sensor ultrasonico y realizar calculos
```

Figure 14 Part of the program code loaded on the Arduino Mega card
Source: Own Elaboration

Development of the application on the Smartphone

In order to create our app we use the open source software called APP INVENTOR. It is only necessary to be connected to the Internet (Wifi) in order to use the inventor App, create an account in Gmail and have an Android device that uses the same Wifi network. The route to enter and use the software is:

http://ai2.appinventor.mit.edu.

The programs are done intuitively using blocks, which are a kind of "puzzle" pieces. It has no source program written in text.

App Inventor appeared on July 12, 2010, and was opened to the public on December 15, 2010. It was developed between Hal Abelson of MIT and Google engineers Ellen Spertus and Liz Looney, along with David Wolber professor of USFCA and developer of the application.

At the beginning of August 2011, Google announced that it would no longer maintain this application, but that it would make it open source for education.

A week later, the Massachusetts Institute of Technology (MIT), a private higher education institution located in Cambridge, Massachusetts (USA), announced that it would take over the project.
In December 2013, MIT released AI 2, a new version of App Inventor.

In November 2014, the language option comes out, which allows us to see most of the elements in Spanish.

The Inventor App is not a program that has to be downloaded to the computer.

ISSN: 2414- 4924

It works in cloud computing (the cloud), the program works by connecting to the Internet and works directly connected to the App Inventor server. It's like a web page and operations are carried out in it; you only need a Gmail account.

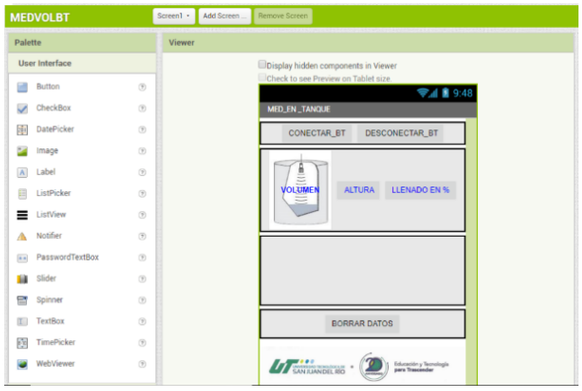

Figure 15 Development of the screen for the application of variable monitoring.
Source: Own Elaboration

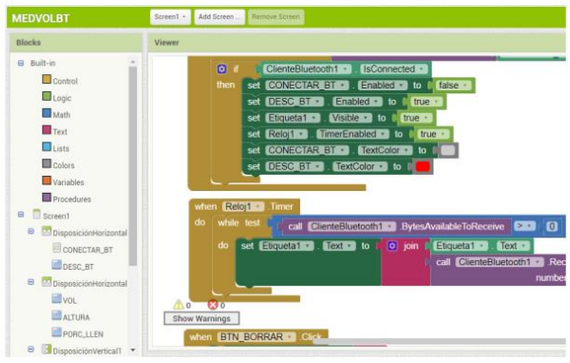

Figure 16 Part of the code that was edited in the programming block editor
Source: Own Elaboration

Figure 17 Information unfolding in app app on phone and LCD display
Source: Own Elaboration

Figure 18 Application app screen on smartphone
Source: Own Elaboration

Formulas used

The echo time of the ultrasonic signal is obtained as a result of the division between two of the time inverted by the sound that travels back and forth from the sensor to the surface of the fluid. The calculation of the average time of the echo (μs), result of the averaged sum of the 50 samples made every 0.5 seconds, is subjected to rounding by the instruction round:

$$tiempo\_eco = round(\frac{tiempo\_eco}{50}) \quad (2)$$

For the calculation of the distance (m) between the sensor and the fluid surface, considering the speed of sound:

$$distancia = tiempo\_eco * 0.0003432 \quad (3)$$

The height of the fluid level (cm) contained in the cylindrical bucket is calculated, also taking into account the thickness of the cork disk float:

$$altura = altura_{max} - (distancia * 100 + corcho) \quad (4)$$

The conversion factor of 1 liter must be taken into account = 1000 cm^3.

We calculate the volume (lts) that displaces the PVC tube as the level of the fluid in the container increases, considering the outside radius and the inside radius to obtain the area of the thickness of the PVC pipe:

ISSN: 2414- 4924

$$volumen_{tubo} = (\pi * 2.5^2 - \pi * 2.3^2) * altura/1000 \quad (5)$$

The volume (lts) of the fluid contained in the tank is calculated, taking into account the inner radius of the tank, the height of the liquid, as well as the volume displaced by the PVC pipe and the initial 3 liter tare already contained in the tank bucket:

$$volumen = \frac{\pi * radio^2 * altura}{1000} - volumen\ tubo + tara \quad (6)$$

Finally, the filling percentage is calculated based on the maximum volume of 15 liters to be in the bucket:

$$porcentaje = \frac{volumen * 100}{15} \quad (7)$$

Tests and results

To carry out the tests, a graduated beaker was used to pour one liter of water into the container, and a graduated scale was stuck inside the tank to obtain a reading of the fluid height level (water) mention that we tried to have the correct leveling of both the table where the bucket was placed and other elements, for this the classic bubble level was used.

Measurements with the rule entail the error of parallelism, this when measuring the height of the surface of the water to determine the height of the level, we must also consider the range of variation of +/- 3mm of the ultrasonic sensor HC-SR04, as well as the variability of the propagation of the speed of sound as a function of the temperature of the environment and relative humidity.

All the aforementioned allows us to understand the reason for the variations and inaccuracies of the experimental results.

Below, we present a table of the measurements of the publications made, as well as the calculations generated by the system based on the Arduino platform.

Table of experimental measurements							
Fluid volume poured into a container with graduated pipette, without tare (liters)	Measured Eco time (microseconds)	Distance to the surface of the fluid quantified with ultrasonic sensor - Arduino (cm)	Fluid level height calculated with Arduino (cm)	Fluid level height measured with graduation (cm)	Absolute height error (calculated - measured) (cm)	Fluid volume calculated with Arduino + tare (liters)	Container filling percentage of 15 liters maximum calculated with Arduino (%)
0	934	32.00	0.00	0.00	0.00	3.04	20.27
1	886	30.40	1.78	1.70	0.08	4.09	27.59
2	836	28.69	3.43	3.60	0.17	5.02	33.58
3	789	27.04	5.01	5.40	0.39	6.22	41.34
4	748	25.67	6.38	7.20	0.82	7.10	47.34
5	699	23.96	7.89	8.80	0.91	8.18	54.51
6	651	22.34	9.71	10.50	0.79	9.23	61.53
7	603	20.69	11.36	12.20	0.84	10.26	68.40
8	556	19.08	12.97	13.80	0.83	11.38	75.28
9	511	17.54	14.55	15.40	0.85	12.28	81.86
10	464	15.92	16.13	16.90	0.77	13.31	88.74
11	419	14.38	17.67	18.50	0.83	14.32	95.47
12	374	12.84	19.21	20.30	1.09	15.29	102.05
Note: tare of 3 liters of fluid (clean water).							

Table 1 Experimental Results
Source: Own Elaboration

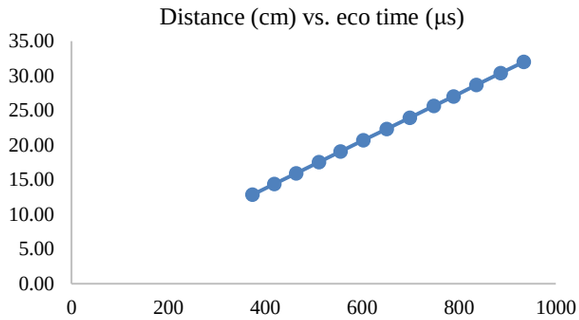

Graphic 1 of data obtained according to Table 1
Source: Own Elaboration

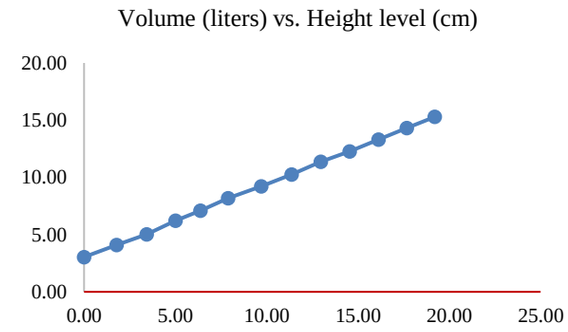

Graphic 2 of data obtained according to Table 1
Source: Own Elaboration

The results denote that there is a margin of variability between what was calculated and measured as regards mainly the height of the fluid level contained in the cuvette, with an average of 0.7 cm of error. Which we consider is not significant for the height of the level shown and monitored; however, these variations in height do affect the results of the volumes calculated, showing an increase in the volumetric value on average of 0.22 liters above the real value of water poured with the beaker.

ISSN: 2414- 4924

In the previous graphs, a linearly acceptable behavior of the different variables measured and calculated is observed.

Figure 19 Container with terminal strip, PVC tube with ultrasonic sensor and graduated beaker
Source: Own Elaboration

Conclusions

Once the present project has been carried out and the results obtained have been evaluated, the following conclusions can be expressed. The system was functional and considering its margin of error, it is acceptable for the experimental purposes of this prototype, the main factors that generate deviations in the accuracy of the results are that the first float is spherical and therefore the rebound of the ultrasonic signals probably not entirely uniform, so we chose the float cylindrical cork disk; the float has oscillations of its height when the fluid is added or removed quickly, so that we must wait for the surface of the water to settle down a little; there are errors inherent in the measurement, such as the volume of fluid that displaces the same PVC tube as more water is added to the container, the small variability in the time measurement of the echo signal of the ultrasonic sensor, the small irregularities of the container of water, the dimensional measurement errors of the container and its height.

The monitoring of the variables height of the fluid level, fluid volume and percentage of filling by the Smartphone has a limited scope due to the maximum distance inherent to communication via Bluetooth (10 m maximum), but meets the expectations of having a remote process monitoring safely.

If another type of fluid level height sensor is used with greater reliability and accuracy, it can be connected to the Arduino Mega - Bluetooth card system and achieve the desired remote monitoring with the smartphone. But it should be mentioned that commercial ultrasonic level sensors for industrial use are around the price of over $ 500, and in this developed system its price was around $ 50, a tenth of the cost.

The system was developed on a small scale of measurement, no more than 30 cm high fluid level and a capacity of 15 liters; but it can be extrapolated to larger measurements that do not exceed 4 m (limitations of the range of the ultrasonic sensor used), with the adjustments in regard to the height sensor of the fluid level.

Finally, considering the cost-benefit relationship, we can conclude that the present prototype fully met the objective.

References

(s.f.). Recuperado el 07 de 2018, de http://www.juntadeandalucia.es/averroes/centros-tic/21700290/helvia/sitio/upload/tema_app_inventor.pdf

(s.f.). Recuperado el 07 de 2018, de www.bkargado.blogspot.com

Chile), I. M. (s.f.). *Arduino.cl*. Recuperado el 07 de 2018, de http://arduino.cl/arduino-mega-2560/

Clark, A. (30 de 12 de 2013). *MIT NEWS*. Obtenido de http://news.mit.edu/2013/app-inventor-launches-second-iteration

DULHOSTE, J.-F. (19 de 2 de 2008). *http://webdelprofesor.ula.ve/ingenieria.* Obtenido de http://webdelprofesor.ula.ve/ingenieria/djean/index_archivos/Documentos/I4_Medicion_de_nivel.pdf

ISSN: 2414- 4924

E direct. (s.f.). Recuperado el 07 de 2018, de https://www.e-direct.endress.com/mx/es/Medici%C3%B3n-de-nivel-por-radar-sin-contacto-Micropilot-FMR10#tab3

etools. (10 de 07 de 2018). Obtenido de http://www.electrontools.com/Home/WP/2016/04/01/como-funciona-el-sensor-ultrasonico-hc-sr04/

GAMA MORENO, L. A., & SANCHEZ RODRIGUEZ, M. A. (1 de 02 de 2010). Diseño De una interfaz para detección de fugas de agua. *Revista Digital Universitaria, 11*(2).

GARCÍA GÓMEZ , O. A., & MOLINA BARRERA, M. A. (2016). PROTOTIPO DE UN SENSOR DE NIVEL LÁSER. CDMX, MEXICO: IPN.

GEEK FACTORY. (s.f.). Recuperado el 07 de 2018, de https://www.geekfactory.mx/tienda/sensores/hc-sr04-sensor-de-distancia-ultrasonico/

GEEK FACTORY. (s.f.). Recuperado el 07 de 2018, de https://www.geekfactory.mx/tutoriales/bluetooth-hc-05-y-hc-06-tutorial-de-configuracion/

Gutiérrez , J., & Porta, G. M. (2018). Medidor ultrasónico de nivel de agua para estanques. *Ingeniería, investigación y tecnología, 7*(4). Obtenido de http://www.scielo.org.mx/scielo.php?script=sci_arttext&pid=S1405-77432006000400004&lng=es&tlng=es.

instructables. (s.f.). Recuperado el 07 de 2018, de https://www.instructables.com/id/Arduino-AND-Bluetooth-HC-05-Connecting-easily/

Lajara Vizcaíno, J. R., & Pelegrí Sebastiá, J. (2014). *Sistemas Integrados con Arduino.* Ciudad de México: Alafaomega.

Microkits Electrónica. (s.f.). Recuperado el 07 de 2018, de https://www.microkitselectronica.com/media/attachment/file/h/c/hcsr04.pdf

MIT. (s.f.). *appinventor.org*. Obtenido de http://www.appinventor.org/content/CourseInABox/Intro/IHaveADream

Omega a spectris company. (s.f.). Recuperado el 07 de 2018, de https://mx.omega.com/pptst/LVU800.html

Reyes Cortés , F., & Cid Monjaraz, J. (2015). *Arduino, aplicaciones en robótica, mecatrónica e ingenierías.* Ciudad de México: Alfaomega.

Saber es práctico. (s.f.). Recuperado el 07 de 2018, de www.saberespractico.com

Tojeiro Calaza, G. (2015). *Taller de Arduino, un enfoque práctico para principiantes.* Ciudad de México, México: Alfaomega.

Wikipedia free encyclopedia. (s.f.). Recuperado el 07 de 2018, de https://es.wikipedia.org/wiki/Vasos_comunicantes

ISSN: 2414- 4924

Article **ECORFAN Journal Democratic Republic of Congo**
June 2018 Vol.4 No.6 29-36

Design and implement a solar tracker control algorithm for a photovoltaic module

Diseñar e implementar un algoritmo de control para el seguimiento solar de un módulo fotovoltaico

AVALOS-GALINDO, Carlos David†, ONTIVEROS-MIRELES, Joel Josué*, GALÁN-HERNÁNDEZ, Néstor Daniel and RUBIO-ASTORGA, Guillermo Javier

Tecnológico Nacional de México/Instituto Tecnológico de Culiacán

ID 1st Author: *Carlos David, Avalos-Galindo* / **ORC ID**: 0000-0002-8660-5021, **Researcher ID Thomson**: H-6582-2018, **Open ID**: 114300923759279285131, **CVU CONACYT ID**: 903133

ID 1st Coauthor: *Joel Josué, Ontiveros-Mireles* / ORC ID: 0000-0002-3717-5141, **Researcher ID Thomson**: H-5429-2018, **Open ID**: 101358849298461976839, **CVU CONACYT ID**: 564321

ID 2nd Coauthor: *Néstor Daniel, Galán-Hernández* / **ORC ID**: 0000-0002-5270-4187, **Researcher ID Thomson**: H-5497-2018, **Arxiv ID**: 0000-0002-5270-4187, **CVU CONACYT ID**: 48401

ID 3rd Coauthor *Guillermo Javier, Rubio-Astorga* / **ORC ID**: 0000-0003-3440-9958, **Researcher ID Thomson**: H-4783-2018, **Open ID**: 116048027903907523090, **CVU CONACYT ID**: 94895

Received January 18, 2018; Accepted June 20, 2018

Abstract

This paper presents the design of two control algorithms, for a one-axis and a tow-axis solar tracker. The solar position with a time correction through the Yallop's algorithm is estimated, in order to define the turn's freedom of the trackers. The mathematical model of the position's system and the mechanical structure of the solar trackers are obtained and two PID controllers are designed through the second tuning method of Ziegler-Nichols. The PID controllers designed are implemented in a microcontroller. This has a visualization stage, power stage, actuators and power and position sensors to close a control loop. The results that are obtained show that it is possible to maintain the output power of a photovoltaic module between a desired range when a solar tracker control algorithm is implemented.

Solar Position, Mathematical Model, Controller

Resumen

En este trabajo se presenta el diseño de dos algoritmos de control para seguidores de uno and dos ejes de libertad. Se estima la posición solar con una corrección de tiempo mediante el algoritmo de Yallop, con la finalidad de determinar la libertad de giro de los seguidores. Se obtiene el modelo matemático del sistema de posicionamiento and de la estructura mecánica de los seguidores solares and se diseñan dos controladores PID, mediante el segundo método de sintonía de Ziegler-Nichols. Los controladores PID diseñados se implementan en un microcontrolador con el desarrollo de las etapas de visualización de datos, acondicionamiento de señal, potencia, actuadores, sensores de potencia and posición solar para cierre del lazo de control. Los resultados que se obtienen muestran que es posible mantener la potencia de salida de un módulo fotovoltaico dentro de un rango de funcionamiento deseado al implementar un algoritmo de control para el seguimiento solar.

Posición Solar, Modelo Matemático, Controlador

Citation: AVALOS-GALINDO, Carlos David, ONTIVEROS-MIRELES, Joel Josué, GALÁN-HERNÁNDEZ, Néstor Daniel and RUBIO-ASTORGA, Guillermo Javier. Design and implement a solar tracker control algorithm for a photovoltaic module. ECORFAN Journal-Democratic Republic of Congo. 2018, 4-6: 29-36.

* Correspondence to Author (email: joelontiveros@itculiacan.edu.mx)
† Researcher contributing first author.

Introduction

Within the renewable energies, photovoltaic energy stands out. This is due to its independence from fossil fuels and low impact on the environment, it is positioned as an ecological alternative to counteract environmental problems that cause the generation of conventional energies (Faria and others, 2017). However, the efficiency of these systems is a matter of great concern among scientists, this is due to the losses by conversion of solar energy to electrical and environmental conditions, such as humidity, dust, shadows, temperature, angle and intensity of incident solar radiation (Sreewirote, 2017).

There are two types of photovoltaic, fixed and mobile systems. The fixed installations have an orientation and inclination depending on the place of installation. Within the mobiles, there are the solar trackers of an axis and of two axes. The first follow the movement of the sun from east to west and increase energy production by 20% compared to fixed installations. The second, in addition to following the solar position from east to west, also follow the solar height, so they increase energy production by 40% compared to fixed installations (Diaz & Carmona, 2015).

Current followers use algorithms that seek to position the horizontal energy capture surface to solar radiation. For example, in (Huynh & Dunnigan, 2016) and (Makhija, Khatwani, Khan, Goel & Roja, 2017), light sensors are used to determine the position of the surface, or in (Astanto, Prasetyandi, Purwadianta & Sambada, 2016), GPS technology is implemented to determine the position of the sun and to orient the catchment surface. However, these jobs do not have a feedback to control the power output of the system.

Unlike previous works, the design of a control algorithm for solar tracking is proposed; that positions the horizontal photovoltaic module to solar radiation, as long as the output power is below the nominal power of the module. The controller modifies the angle of incidence when the power is between ± 5% of its nominal value, this to keep the production of energy within this range as long as possible.

The purpose of implementing the control is to avoid damage due to overproduction of energy and prolong the useful life of the photovoltaic module.

To determine the solar position and modify the angle of inclination of the module, a light sensor is used; in addition to voltage and current sensors to calculate the output power of the system, in order to obtain feedback and close the PID control loop implemented in a microcontroller.

This work is developed in VIII sections. In section II, the solar position for a given point is estimated. The mathematical model of structures for solar tracking is presented in section III. Section IV describes the design of the PID control algorithm. The simulation graphs are shown in section V, in section VI the implementation is described, in section VII the results are presented, in section VIII the acknowledgments and in section IX the conclusions.

Estimation of solar position

To estimate the position of the sun with respect to the earth, two angles of interest are estimated, the hour angle (ω) and the solar height (α), shown in Figure 1 (Khatib & Elmenraich, 2016). This is done in order to know the freedom of rotation that solar trackers should have.

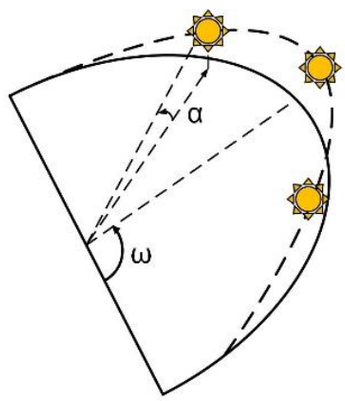

Figure 1 Solar height and hour angle
Source: (Khatib & Elmenraich, 2016)

It is considered that the standard time differs from the true solar time (Tsv), for which a time correction is made by means of the Yallop algorithm. This is chosen for its high precision for the years from 1980 to 2050 (Muneer, Gueymard & Kambezidis, 2004).

ISSN: 2414- 4924

$$T_{sv}=U_T+E_{TC}+\frac{1}{15}(L_{mel}+L_{Long}) \quad (1)$$

Where UT is the time in hours (hrs), ETC is the corrected time equation (hrs), Lmel is the local longitude meridian standard (°) and LLong is the meridian length of the observer (°). The hour angle is defined as the angular displacement of the sun from east to west, taking a local point as a reference. The solar height as the angular height of the sun measured from the horizontal (Muneer, Gueymard & Kambezidis, 2004). These angles are estimated by the equations:

$$\omega = \frac{15T_{sv}-(12\times60)}{60} \quad (2)$$

$$\alpha = \text{asen}[\text{sen}(\varphi)\text{sen}(\delta_{dec}+\cos(\varphi)\cos(\omega) \quad (3)$$

Where φ is the latitude of the installation point in (°), and δ_{dec} is the decline considered at solar noon (°).

Modelado de sistema de seguimiento

The design of the two followers is done in SOLIDWORKS®. The device of an axis of freedom follows the hour angle (ω) with a fixed angle of inclination (β) of 24 ° (Figure 2). The follower of two axes of freedom (Figure 3), acts both for the hour angle (ω) and for the angle of the solar height (α).

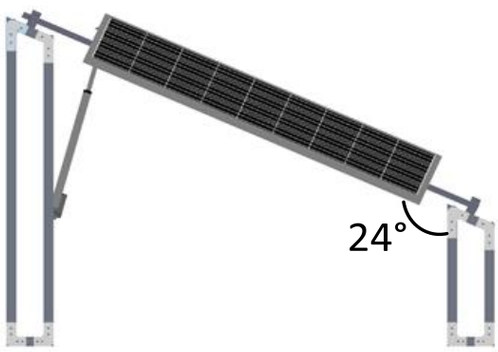

Figure 2 Follower of an axis of freedom
Source: Own Elaboration

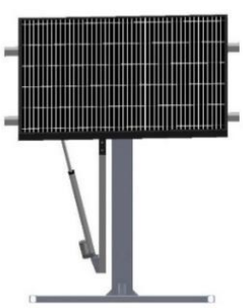

Figure 3 Seguidor solar de dos ejes de libertad
Source: Own Elaboration

The solar tracking system is made up of two parts as shown in Figure 4 (Utkin, Guldner & Shi, 2009). A positioning system and a mechanical system that replaces the mechanical structures shown in Figure 2 and Figure 3, where B1 and B2 represent the bearings, and J the moment of inertia of the photovoltaic module.

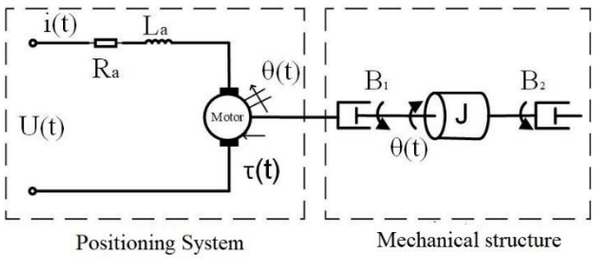

Figure 4 Solar tracking system
Source: Modified from (Utkin, Gundner 6 Shi, 2009) and (Ogata, 2010)

The mathematical model of the positioning system consists of a permanent magnet DC motor, which is governed by two equations, one electrical and one mechanical (Utkin, Guldner & Shi, 2009):

$$U(t)=R_a i(t)+L_a\frac{di(t)}{dt}+K_e\frac{d\theta(t)}{dt} \quad (4)$$

$$\tau(t)=J_1\frac{d^2\theta(t)}{dt}+B\frac{d\theta(t)}{dt} \quad (5)$$

The second law of Newton states that the algebraic sum of moments or pairs around a fixed axis is equal to the product of inertia by angular acceleration, therefore, the mathematical equation of the mechanical structure is (Ogata, 2010):

$$\tau(t)=J\frac{d^2\theta(t)}{dt}+B_1\frac{d\theta(t)}{dt}+B_2\frac{d\theta(t)}{dt} \quad (6)$$

By joining the equations (4), (5) and (6) and eliminating the viscous friction coefficients B1 and B2, we obtain the transfer function of the follower of an axis of freedom:

$$\frac{\theta(s)}{V(s)}=\frac{K_M}{s[(J_1L_a+JL_a)s^2+(J_1R_a+\ldots}$$

$$\overline{\ldots JR_a+BL_a)s+K_MK_e]}$$

AVALOS-GALINDO, Carlos David, ONTIVEROS-MIRELES, Joel Josué, GALÁN-HERNÁNDEZ, Néstor Daniel and RUBIO-ASTORGA, Guillermo Javier. Design and implement a solar tracker control algorithm for a photovoltaic module. ECORFAN Journal-Democratic Republic of Congo. 2018.

Where R_a is the armature resistance (Ω), La is the armature inductance (H), i (t) the armature current (A), θ (t) the position (°), K_e the electromotive force constant, τ (t) the torque, J the moment inertia of the photovoltaic module (Kg), J1 the inertia of the motor rotor (Kg) and B the viscosity coefficient (kg/s). The moment of inertia of the photovoltaic module is obtained by means of equation (8) (Jonhson, Mazurek & Eizanberg, 2010).

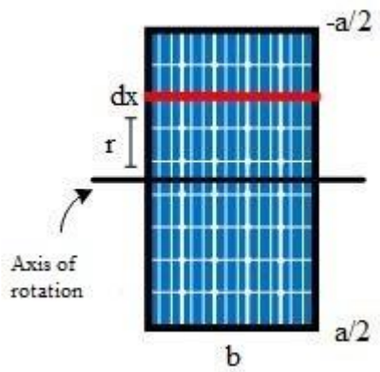

Figure 5 Moment of horizontal inertia.
Source: Own Elaboration

$$J_3=\frac{M_a}{b}\int_{-\frac{a}{2}}^{\frac{a}{2}} x^2\,dx \qquad (8)$$

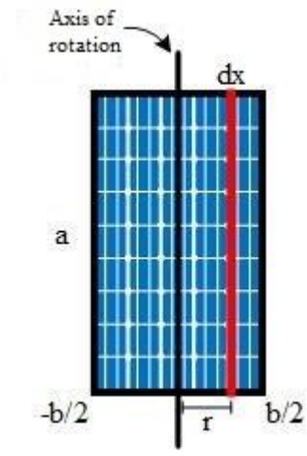

Figure 6 Moment of vertical inertia
Source: Own Elaboration

$$J=\frac{M_a}{b}\int_{-\frac{b}{2}}^{\frac{b}{2}} x^2\,dx \qquad (9)$$

To obtain the mathematical model of the two-axis follower, each axis of freedom is considered as an independent system. In the system of the hour angle tracker, equations (7) and (8) are implemented. For the solar height tracker, equation (7) is considered, where the moment of inertia of the photovoltaic module is obtained with the equation (9).

I. Design of PID control algorithm

A PID controller is designed which is based on the scheme proposed by Ogata (2010), Figure 7. It has 3 tunable parameters, which are the proportional action K_P, the integration time T_i, and the derivation time T_d.

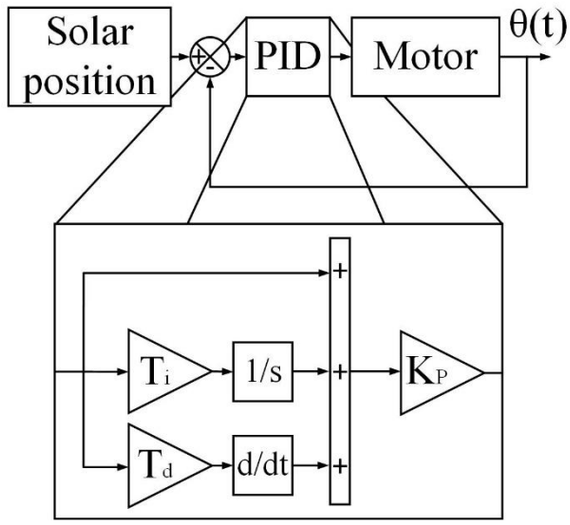

Figure 7 Block diagram of PID controller
Source: (Ogata, 2010)

$$PID= K_P\left(1+\frac{1}{T_i s}+T_d s\right) \qquad (10)$$

The 3 parameters of the PID equation are calculated by means of the second Ziegler Nichols tuning method and equation (7). In addition, a manual tuning is performed to increase its accuracy (Ogata, 2010). The results are shown in Table 1, Table 2, and Table 3.

	Ziegler Nichols	Tuned
K_P	104.848	10.4848
T_i	5.048	0.05048
T_d	1.262	0.001262

Table 1 Hourly angle controller gains for an axis tracker
Source: Own Elaboration

	Ziegler Nichols	Tuned
K_P	235.3547	2.3535
T_i	14.1285	0.1413
T_d	3.5321	0.0035

Table 2 Solar height angle controller gains for two-axis tracker
Source: Own Elaboration

ISSN: 2414- 4924

	Ziegler Nichols	Tuned
K_P	207.6485	2.0765
T_i	11.1032	14.1285
T_d	2.7758	0.0026

Table 3 Winnings of hour angle controller for two-axis tracker
Source: Own Elaboration

Simulations

With equations (1), (2) and (3), the solar height and the hour angle at dawn and sunset are estimated in the MATLAB® programming environment. The results shown in Graph 1 and Graph 2 are obtained.

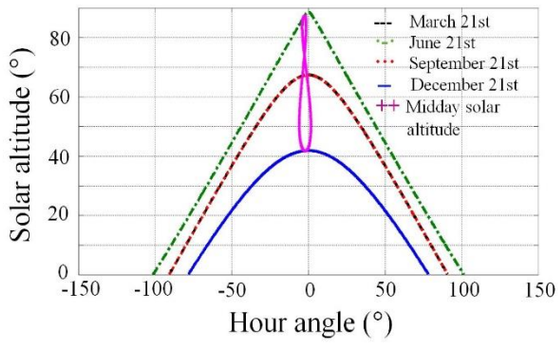

Graphic 1 Estimation of solar height
Source: Own Elaboration

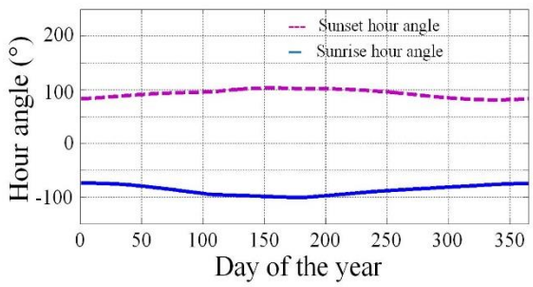

Graphic 2 Estimation of hour angle at dawn and dusk
Source: Own Elaboration

From Graphic 1, it can be seen that one must have a freedom from 0 ° to 90 ° to follow the solar height (90 ° is the horizontal). In Graphic 2, an average angle at sunrise of -87 ° and at nightfall of 92 ° is obtained. It is concluded that it should have an approximate freedom of -90 ° to 90 ° (where 0 ° is the horizontal). Three simulations are carried out in SIMULINK® to know the response of the tracking system according to the diagram shown in Figure 7. Equations (1), (2) and (3) are used to know the solar position, (8) for system dynamics and (10) together with Table 1, Table 2 and Table 3 for the PID controller

The results shown in Graphic 3, Graphic 4 and Graphic 5 are obtained.

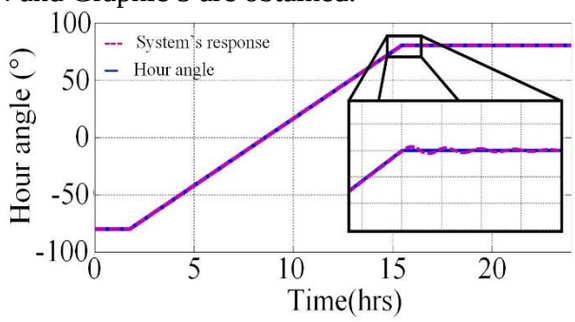

Graphic 3 Follower controller response to an axis of freedom
Source: Own Elaboration

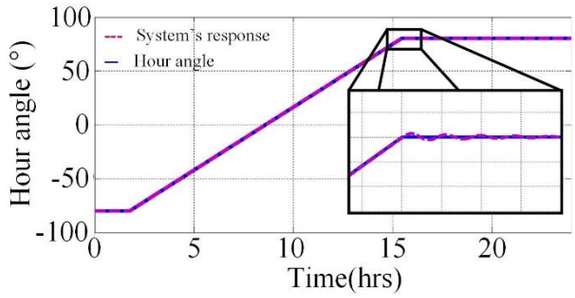

Graphic 4 Time angle controller response for two-axis freedom tracker
Source: Own Elaboration

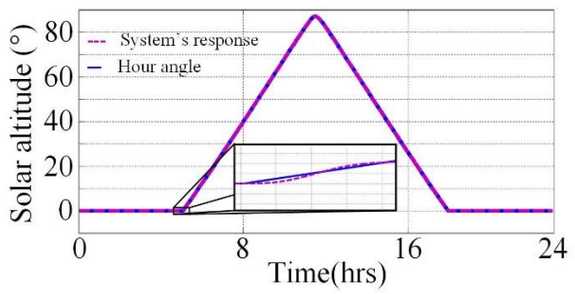

Graphic 5 Solar height controller response for two axis of freedom tracker
Source: Own Elaboration

Graphic 3, Graphic 4 and Graphic 5 show the tracking systems that are modeled, are able to follow the trajectory of the solar height and the hour angle.

Implementation

The implementation of the solar tracking algorithm is based on the block diagram of Figure 8.

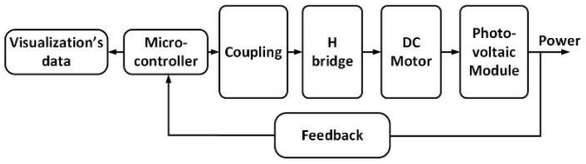

Figure 8 Implementation diagram
Source: Own Elaboration

ISSN: 2414- 4924

The data display stage uses a 16x2 LCD screen, which shows the feedback variables such as: electric current (Honeywall, 2018), voltage, and radiation. A 16F2550 microcontroller (Microchip, 2004) is used, where the control algorithm (10) is programmed. For the control and power coupling stage, optocouplers 4N25 (TOSHIBA, 1998) and 2N2222A transistors (Semicon, 2013) are used.

A bridge H (Hart, 2011) with TIP31C transistors is designed to control the rotation of the XLA18 engine of the positioning system. In the follower of an axis a polycrystalline module is used and in the one of two axes an amorphous one, its specifications are shown in Table 4.

Parameter	Polycrystalline module	Amorphous module
P_{mp}	250W	135W
V_{mp}	30.2V	62.3V
I_{mp}	8.3A	2.17A
V_{oc}	37.8V	78.4V
I_{sc}	8.7A	2.52A

Table 4 Module specifications
Source: Own Elaboration

To measure the power produced by the photovoltaic module, the CSNE151 current sensor and the LV25P voltage sensor are used. To determine the solar position a light sensing device similar to that presented in (Huynh & Dunnigan, 2016), (Majhija, Khatwani, Khan, Goel & Roja, 2017) and as shown in the sample in Figure 9 is designed.

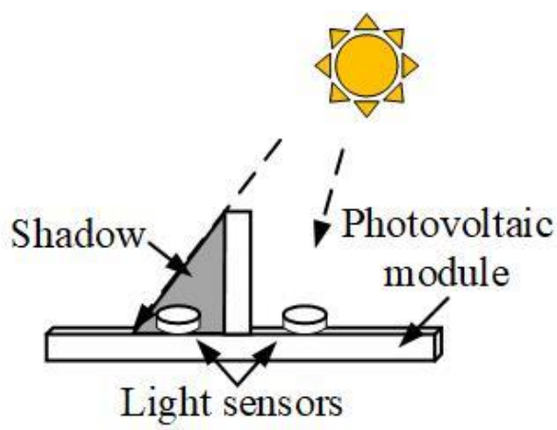

Figure 9 Solar position sensor
Source: Own Elaboration

Results

Test 1

The objective of test 1 is to maintain the power of the amorphous photovoltaic module mounted on the two-axis follower by ± 5% its nominal power. The data sampling process is carried out on June 1 with a duration of 12 hours (7:00 a.m. to 7:00 p.m.), period in which power measurements are taken every 10min. The results are shown in Graphic 6.

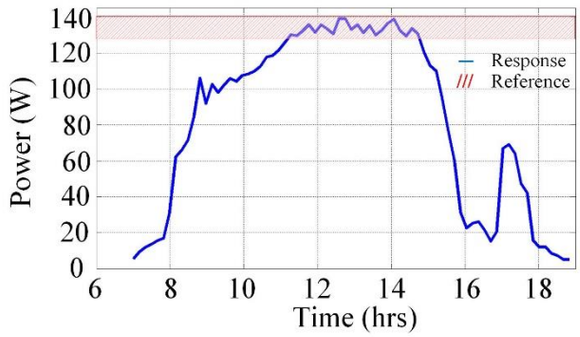

Graphic 6 Test results 1
Source: Own Elaboration

Test 2

The objective of test 2 is to maintain the power of the amorphous photovoltaic module following a reference power. It is chosen randomly on June 2. The data sampling process lasts 10 hours (8:00 a.m. to 6:00 p.m.), period in which power measurements are made every 10min. The results are shown in Graphic 7.

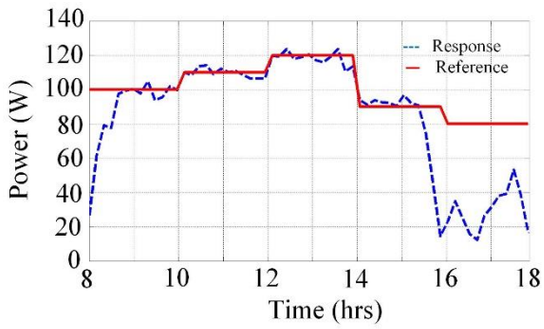

Graphic 7 Test results 2
Source: Own Elaboration

ISSN: 2414- 4924

Test 3

The objective of test 3 is to maintain the power of the polycrystalline photovoltaic module mounted on the follower of an axis in ± 5% of its nominal power from 9:00 am to 2:00 pm, from this time until 6:00 pm change the reference. It is chosen randomly on June 5. The data sampling process is for a period of 10 hours (9:00 a.m. to 6:00 p.m.), in which power measurements are made every 10min. The results shown in Graphic 8 are obtained.

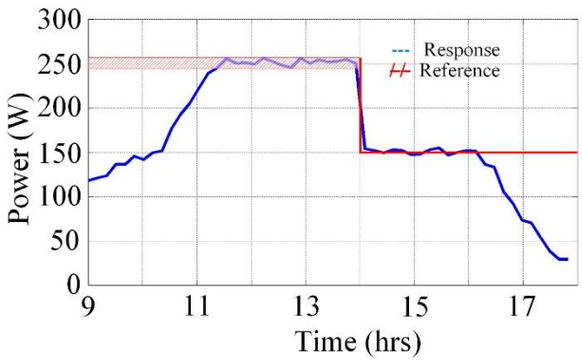

Graphic 8 Test results 3
Source: Own Elaboration

Acknowledgement

To the National Technologic of Mexico for the support they provided to the project "Development and characterization of the solar resource for technological applications in renewable energies of the primary sector" with code 6070.17-P.

Conclusions

In the present work, the structures for one and two axes in the SOLIDWORKS® program were designed. In the development of the prototypes, the electrical signals of sensors and actuators were conditioned in order that the 18F2550 microcontroller interprets the data and controls the actuators in an appropriate way. A control algorithm programmed with CCS Compiler® is designed and implemented to read the signals transmitted by the sensors, interpret them and execute the control algorithm that decides the positioning of the photovoltaic modules based on the position of the sun and the power produced.

When analyzing Graphic 6, it can be seen that the photovoltaic module operates within its nominal range for 4hrs, from 11:00 AM to 3:00 PM. In the period from 15:40 to 17:00 hrs, there is an abrupt drop in production, this is due to shadows caused by the vegetation of the point. It is observed in Graphic 7, that the controller is able to make the power produced by the photovoltaic module follow any programmed reference.

In Graphic 8 it is observed in the period from 11:30 a.m. to 2:00 p.m., that the photovoltaic module operates within its nominal range, and from 2:00 p.m. to 4:00 p.m. follows the 150W reference, validating the correct operation of the controller.

It is possible to design a controller for the structure of one and two axes of freedom, which allows to maintain the production of energy within ± 5% of its nominal parameters in the peak hours of the day. It even manages to maintain a power less than the nominal, which opens the doors to these systems are scalable.

References

Astanto, D., Prasetyadi, A., Purwadianta, D., & Sambada, R. (2016). Design of a GPS-Based Solar tracker System for a Vertical Solar Still. ICSGTEIS. Bali.

Diaz Corcobado, T., & Carmona Rubio, G. (2015). Istalaciones solares fotovoltaicas. Madrid, España: Mc Graw Hill.

Faria, F., Domingos, J. L., Junior, J. A., Domingues, E. G., Alves, A. J., Calixto, W. P., & Ferreira, G. b. (2017). Energy Efficiency and Renewable Energy: Energy, Economics and Environment Gains. 2017 IEEE URUCON. Montevideo, Uruguay.

Hart, D. (2011). Power Electronics. Indiana, USA: Mc Graw Hill.

Honeywall. (12 de 05 de 2018). Obtenido de www.farnell.com: http://www.farnell.com/datasheets/797310.pdf

Huynh, D., & Dunnigan, M. (2016). Development and Comparison of an Improved Incremental Conductance Algorithm for Tracking the MPP of a Solar PV Panel. IEEE Transactions on Sustainable Energ, 1421-1429.

ISSN: 2414- 4924

Jonhson, B., Mazurek, & Eizanberg. (2010). Mecánica Vectorial Para Ingenieros: Estática. Ciudad de México, México: Mc Grew Hill.

Khatib, T., & Elmenraich, W. (2016). Modellinf of a Photovoltaic System Using Matlab. Canadá: Woley & Sons, Inc.

Makhija, S., Khatwani, A., Khan, M. F., Goel, V., & Roja, M. (2017). Design & Implementation of an Automated Dual-Axis Solar Tracker with Data-Logging. International Conference on Inventive Systems and control. Mumbai.

Microchip. (2004). Microchip Technology Inc. Obtenido de ww1.microchip.com: http://ww1.microchip.com/downloads/en/DeviceDoc/39632b.pdf

Muneer, T., Gueymard, C., & Kambezidis, H. (2004). Solar Radiation and Daylight Models. Sheffield, England: Butterworth-Heinemann.

Ogata, K. (2010). Ingeniería de Control Moderna. Madrid, España: Pearson Education,
Semicon, O. (11 de 2013). web.mit.edu. Obtenido de http://web.mit.edu/6.101/www/reference/2N2222A.pdf

Sreewirote, B. (2017). Increasing Efficiency of an Electricity Production System from Solar Energy with a Method of Reducing Solar Panel Temperature. 2017 IEEE International Conference on Applied System Innovation. Sapporo, Japón.

TOSHIBA. (1998). TOSHIBA Leading Innovation. Obtenido de www.toshiba.com: https://pdf1.alldatasheet.com/datasheet-pdf/view/30830/TOSHIBA/4N25.html

Utkin, V., Guldner, J., & Shi, J. (2009). Sliding Mode Control in Electro-Mechanical Systems. Columbus, Ohio, USA: Taylor& Francis Group, LLC.

ISSN: 2414- 4924

[Title in Times New Roman and Bold No. 14 in English and Spanish]

Surname (IN UPPERCASE), Name 1st Author†*, Surname (IN UPPERCASE), Name 1st Coauthor, Surname (IN UPPERCASE), Name 2nd Coauthor and Surname (IN UPPERCASE), Name 3rd Coauthor

Institutional Affiliation of Author including Dependency (No.10 Times New Roman and Italic)

International Identification of Science - Technology and Innovation

ID 1st author: (ORC ID - Researcher ID Thomson, arXiv Author ID - PubMed Author ID - Open ID) and CVU 1st author: (Scholar-PNPC or SNI-CONACYT) (No.10 Times New Roman)

ID 1st coauthor: (ORC ID - Researcher ID Thomson, arXiv Author ID - PubMed Author ID - Open ID) and CVU 1st coauthor: (Scholar or SNI) (No.10 Times New Roman)

ID 2nd coauthor: (ORC ID - Researcher ID Thomson, arXiv Author ID - PubMed Author ID - Open ID) and CVU 2nd coauthor: (Scholar or SNI) (No.10 Times New Roman)

ID 3rd coauthor: (ORC ID - Researcher ID Thomson, arXiv Author ID - PubMed Author ID - Open ID) and CVU 3rd coauthor: (Scholar or SNI) (No.10 Times New Roman)

(Report Submission Date: Month, Day, and Year); Accepted (Insert date of Acceptance: Use Only ECORFAN)

Abstract (In English, 150-200 words)

Objectives
Methodology
Contribution

Keywords (In English)

Indicate 3 keywords in Times New Roman and Bold No. 10

Abstract (In Spanish, 150-200 words)

Objectives
Methodology
Contribution

Keywords (In Spanish)

Indicate 3 keywords in Times New Roman and Bold No. 10

Citation: Surname (IN UPPERCASE), Name 1st Author†*, Surname (IN UPPERCASE), Name 1st Coauthor, Surname (IN UPPERCASE), Name 2nd Coauthor and Surname (IN UPPERCASE), Name 3rd Coauthor. Paper Title. ECORFAN Journal-Democratic Republic of Congo. Year 1-1: 1-11 [Times New Roman No.10]

* Correspondence to Author (example@example.org)
† Researcher contributing as first author.

Introduction

Text in Times New Roman No.12, single space.

General explanation of the subject and explain why it is important.

What is your added value with respect to other techniques?

Clearly focus each of its features

Clearly explain the problem to be solved and the central hypothesis.

Explanation of sections Article.

Development of headings and subheadings of the article with subsequent numbers

[Title No.12 in Times New Roman, single spaced and bold]

Products in development No.12 Times New Roman, single spaced.

Including graphs, figures and tables-Editable

In the article content any graphic, table and figure should be editable formats that can change size, type and number of letter, for the purposes of edition, these must be high quality, not pixelated and should be noticeable even reducing image scale.

[Indicating the title at the bottom with No.10 and Times New Roman Bold]

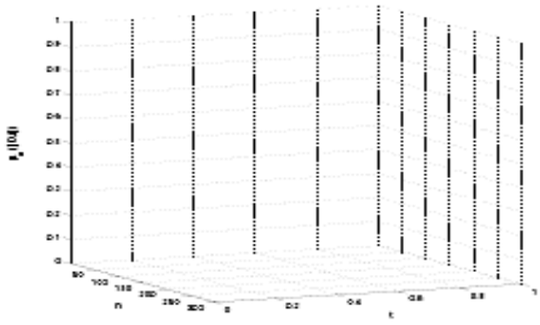

Graphic 1 Title and *Source (in italics)*

Should not be images-everything must be editable.

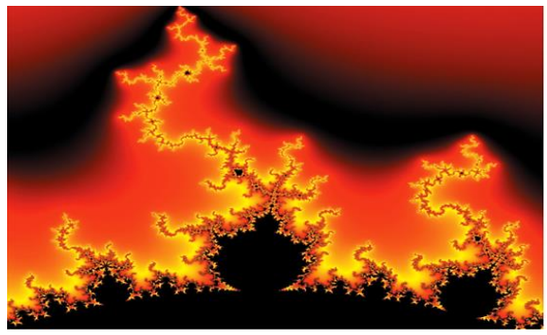

Figure 1 Title and *Source (in italics)*

Should not be images-everything must be editable.

Table 1 Title and *Source (in italics)*

Should not be images-everything must be editable.

Each article shall present separately in **3 folders**: a) Figures, b) Charts and c) Tables in .JPG format, indicating the number and sequential Bold Title.

For the use of equations, noted as follows:

$$Y_{ij} = \alpha + \sum_{h=1}^{r} \beta_h X_{hij} + u_j + e_{ij} \qquad (1)$$

Must be editable and number aligned on the right side.

Methodology

Develop give the meaning of the variables in linear writing and important is the comparison of the used criteria.

Results

The results shall be by section of the article.

Annexes

Tables and adequate sources thanks to indicate if were funded by any institution, University or company.

Conclusions

Explain clearly the results and possibilities of improvement.

ISSN: 2414- 4924

References

Use APA system. Should not be numbered, nor with bullets, however if necessary numbering will be because reference or mention is made somewhere in the Article.

Use Roman Alphabet, all references you have used must be in the Roman Alphabet, even if you have quoted an Article, book in any of the official languages of the United Nations (English, French, German, Chinese, Russian, Portuguese, Italian, Spanish, Arabic), you must write the reference in Roman script and not in any of the official languages.

Technical Specifications

Each article must submit your dates into a Word document (.docx):

Journal Name
Article title
Abstract
Keywords
Article sections, for example:

1. Introduction
2. Description of the method
3. Analysis from the regression demand curve
4. Results
5. Thanks
6. Conclusions
7. References

Author Name (s)
Email Correspondence to Author
References

Intellectual Property Requirements for editing:

-Authentic Signature in Color of Originality Format Author and Coauthors

-Authentic Signature in Color of the Acceptance Format of Author and Coauthors

ISSN: 2414- 4924

Reservation to Editorial Policy

ECORFAN-Democratic Republic of Congo reserves the right to make editorial changes required to adapt the Articles to the Editorial Policy of the Journal. Once the Article is accepted in its final version, the Journal will send the author the proofs for review. ECORFAN® will only accept the correction of errata and errors or omissions arising from the editing process of the Journal, reserving in full the copyrights and content dissemination. No deletions, substitutions or additions that alter the formation of the Article will be accepted.

Code of Ethics - Good Practices and Declaration of Solution to Editorial Conflicts

Declaration of Originality and unpublished character of the Article, of Authors, on the obtaining of data and interpretation of results, Acknowledgments, Conflict of interests, Assignment of rights and Distribution

The ECORFAN-Mexico, S.C Management claims to Authors of Articles that its content must be original, unpublished and of Scientific, Technological and Innovation content to be submitted for evaluation.

The Authors signing the Article must be the same that have contributed to its conception, realization and development, as well as obtaining the data, interpreting the results, drafting and reviewing it. The Corresponding Author of the proposed Article will request the form that follows.

Article title:

- The sending of an Article to ECORFAN-Democratic Republic of Congo emanates the commitment of the author not to submit it simultaneously to the consideration of other series publications for it must complement the Format of Originality for its Article, unless it is rejected by the Arbitration Committee, it may be withdrawn.

- -None of the data presented in this article has been plagiarized or invented. The original data are clearly distinguished from those already published. And it is known of the test in PLAGSCAN if a level of plagiarism is detected Positive will not proceed to arbitrate.

- References are cited on which the information contained in the Article is based, as well as theories and data from other previously published Articles.

- The authors sign the Format of Authorization for their Article to be disseminated by means that ECORFAN-Mexico, S.C. In its Holding Democratic Republic of Congo considers pertinent for disclosure and diffusion of its Article its Rights of Work.

- Consent has been obtained from those who have contributed unpublished data obtained through verbal or written communication, and such communication and Authorship are adequately identified.

- The Author and Co-Authors who sign this work have participated in its planning, design and execution, as well as in the interpretation of the results. They also critically reviewed the paper, approved its final version and agreed with its publication.

- No signature responsible for the work has been omitted and the criteria of Scientific Authorization are satisfied.

- The results of this Article have been interpreted objectively. Any results contrary to the point of view of those who sign are exposed and discussed in the Article.

Copyright and Access

The publication of this Article supposes the transfer of the copyright to ECORFAN-Mexico, SC in its Holding Democratic Republic of Congo for its ECORFAN-Democratic Republic of Congo, which reserves the right to distribute on the Web the published version of the Article and the making available of the Article in This format supposes for its Authors the fulfilment of what is established in the Law of Science and Technology of the United Mexican States, regarding the obligation to allow access to the results of Scientific Research.

Article Title:

Name and Surnames of the Contact Author and the Coauthors	Signature
1.	
2.	
3.	
4.	

Principles of Ethics and Declaration of Solution to Editorial Conflicts

Editor Responsibilities

The Publisher undertakes to guarantee the confidentiality of the evaluation process, it may not disclose to the Arbitrators the identity of the Authors, nor may it reveal the identity of the Arbitrators at any time.

The Editor assumes the responsibility to properly inform the Author of the stage of the editorial process in which the text is sent, as well as the resolutions of Double-Blind Review.

The Editor should evaluate manuscripts and their intellectual content without distinction of race, gender, sexual orientation, religious beliefs, ethnicity, nationality, or the political philosophy of the Authors.

The Editor and his editing team of ECORFAN® Holdings will not disclose any information about Articles submitted to anyone other than the corresponding Author.

The Editor should make fair and impartial decisions and ensure a fair Double-Blind Review.

Responsibilities of the Editorial Board

The description of the peer review processes is made known by the Editorial Board in order that the Authors know what the evaluation criteria are and will always be willing to justify any controversy in the evaluation process. In case of Plagiarism Detection to the Article the Committee notifies the Authors for Violation to the Right of Scientific, Technological and Innovation Authorization.

Responsibilities of the Arbitration Committee

The Arbitrators undertake to notify about any unethical conduct by the Authors and to indicate all the information that may be reason to reject the publication of the Articles. In addition, they must undertake to keep confidential information related to the Articles they evaluate.

Any manuscript received for your arbitration must be treated as confidential, should not be displayed or discussed with other experts, except with the permission of the Editor.

The Arbitrators must be conducted objectively, any personal criticism of the Author is inappropriate.

The Arbitrators must express their points of view with clarity and with valid arguments that contribute to the Scientific, Technological and Innovation of the Author.

The Arbitrators should not evaluate manuscripts in which they have conflicts of interest and have been notified to the Editor before submitting the Article for Double-Blind Review.

Responsibilities of the Authors

Authors must guarantee that their articles are the product of their original work and that the data has been obtained ethically.

Authors must ensure that they have not been previously published or that they are not considered in another serial publication.

Authors must strictly follow the rules for the publication of Defined Articles by the Editorial Board.

The authors have requested that the text in all its forms be an unethical editorial behavior and is unacceptable, consequently, any manuscript that incurs in plagiarism is eliminated and not considered for publication.

Authors should cite publications that have been influential in the nature of the Article submitted to arbitration.

Information services

Indexation - Bases and Repositories

RESEARCH GATE (Germany)
GOOGLE SCHOLAR (Citation indices-Google)
REDIB (Ibero-American Network of Innovation and Scientific Knowledge- CSIC)
MENDELEY (Bibliographic References Manager)

Publishing Services:

Citation and Index Identification H.
Management of Originality Format and Authorization.
Testing Article with PLAGSCAN.
Article Evaluation.
Certificate of Double-Blind Review.
Article Edition.
Web layout.
Indexing and Repository
ArticleTranslation.
Article Publication.
Certificate of Article.
Service Billing.

Editorial Policy and Management

244 – 2 Itzopan Street La Florida, Ecatepec Municipality Mexico State, 55120 Zipcode, MX. Phones: +52 1 55 2024 3918, +52 1 55 6159 2296, +52 1 55 4640 1298; Email: contact@ecorfan.org www.ecorfan.org

Management Offices
244 Itzopan, Ecatepec de Morelos–México.
21 Santa Lucía, CP-5220. Libertadores -Sucre–Bolivia.
38 Matacerquillas, CP-28411. Moralzarzal –Madrid-España.
18 Marcial Romero, CP-241550. Avenue, Salinas l - Santa Elena-Ecuador.
1047 La Raza Avenue -Santa Ana, Cusco-Peru.
Boulevard de la Liberté, Immeuble Kassap, CP-5963.Akwa- Douala-Cameroon.
Southwest Avenue, San Sebastian – León-Nicaragua.
6593 Kinshasa 31 – Republique Démocratique du Congo.
San Quentin Avenue, R 1-17 Miralvalle - San Salvador-El Salvador.
16 Kilometro, American Highway, House Terra Alta, D7 Mixco Zona 1-Guatemala.
105 Alberdi Rivarola Captain, CP-2060. Luque City- Paraguay.
YongHe district, ZhongXin, Street 69. Taipei-Taiwan.

ECORFAN Journal-Democratic Republic of Congo

2414 4924
ISSN 2414 - 4924

www.ecorfan.org